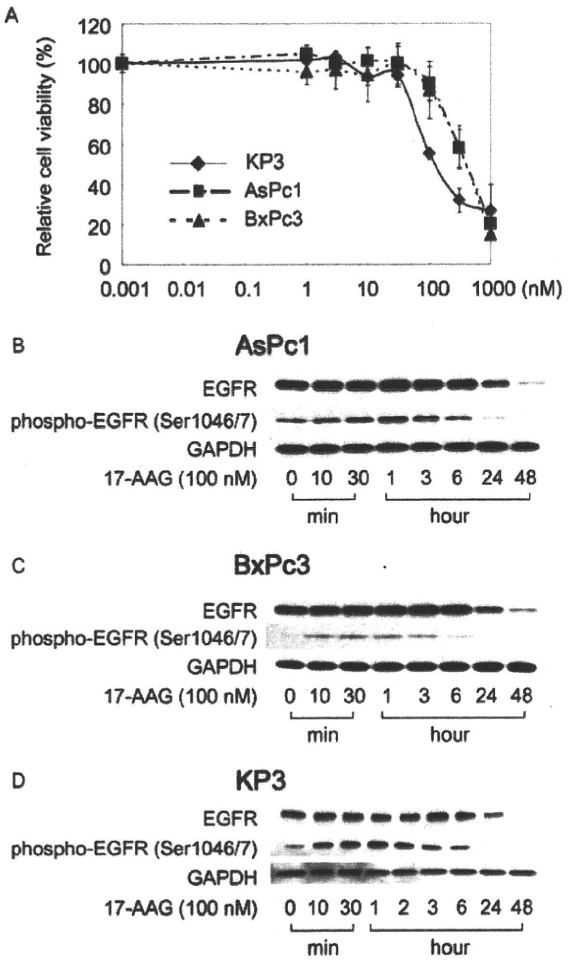

Figure 1. (A) Inhibition of cell growth by 17-AAG in pancreatic cancer cells. Cell viability assay was performed using the MTT cell proliferation kit I. Results are expressed as percentage of growth with 100% representing control cells treated with vehicle alone. Bars designate SD of triplicate assays. (B-C) 17-AAG caused desensitization of EGFR and phosphorylation of EGFR at Ser1046/7 in KP3 (A), BxPc3 (B) and AsPc1 (C) pancreatic cancer cells. The indicated cells were treated with 17-AAG at a dose of 100 nM, respectively, for the indicated periods and protein extracts were then harvested and examined by Western blotting using anti-EGFR, anti-phospho-EGFR at Ser1046/7 and anti-GAPDH antibodies.

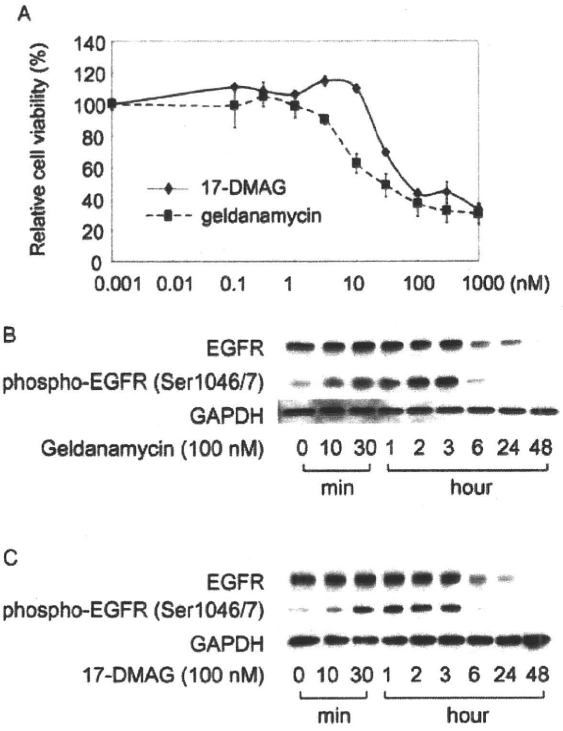

Figure 2. (A) Geldanamycin and 17-DMAG caused inhibition of cell growth in KP3 pancreatic cancer cells. Cell viability assay was performed using the MTT cell proliferation kit I. Results are expressed as percentage of growth with 100% representing control cells treated with vehicle alone. Bars designate SD of triplicate assays. (B) Geldanamycin and 17-DMAG caused desensitization of EGFR and phosphorylation of EGFR at Ser1046/7 in KP3 pancreatic cancer cells KP3 cells were treated with the indicated compounds at a dose of 100 nM, respectively, for the indicated periods and protein extracts were then harvested and examined by Western blotting using anti-EGFR, anti-phospho-EGFR at Ser1046/7 and anti-GAPDH antibodies.

shown in Fig. 1A, the IC_{50} values of 17-AAG in KP3 cells was 70 nM, whereas those in BxPc3 and AsPc1 were 300 and 400 nM, respectively. These results suggest that 17-AAG has potent anti-cancer effect in pancreatic cancer cells.

17-AAG caused desensitization of EGFR, concurrently inducing phosphorylation of EGFR at Ser1046/7 in pancreatic cancer cells. We next examined the effect of 17-AAG on the desensitization of EGFR in these pancreatic cancer cells. As shown in Fig. 1B-D, when the cells were treated with 17-AAG, the protein level of EGFR was time-dependently decreased, respectively (Fig. 1B-D, upper panels). In addition, we examined the effects of 17-AAG on the phosphorylation of EGFR at Ser1046/7, since this phosphorylation has been reported to play an important role in EGFR desensitization (20,25). Interestingly, 17-AAG induced phosphorylation of EGFR at Ser1046/7 at a peak of 30 min to 1 h (Fig. 1B-D, middle panel, respectively). Significant effect by 17-AAG on this phosphorylation was observed within 10 min in these types of pancreatic cancer cells. Since EGFR proteins were concurrently decreased, it seems that phosphorylation of EGFR at Ser1046/7 induced by 17-AAG correlates with its desensitization in these pancreatic cells.

Other HSP90 inhibitors also caused EGFR desensitization concurrently inducing phosphorylation of EGFR at Ser1046/7. To prove that these results (Fig. 1) are not confined to 17-AAG, we examined the effects of geldanamycin and 17-DMAG as other HSP90 inhibitors on cytotoxicity and desensitization of EGFR. We performed a cell proliferating assay using MTT in KP3 pancreatic cells and found that geldanamycin as well as 17-DMAG exerted similar effects on cytotoxicity (IC_{50}; 30 and 100 nM, respectively) in KP3 cells (Fig. 2A). In addition, treatment of the cells with either 100 nM of geldanamycin or 17-DMAG for 6 h resulted in significant decrease in EGFR protein level (Fig. 2B and C, upper panel, respectively). Moreover, treatment of the cells with geldanamycin or 17-DMAG induced phosphorylation of EGFR at Ser1046/7 at a peak of 30 min to 3 h (Fig. 2B and C, middle panel, respectively). Therefore,

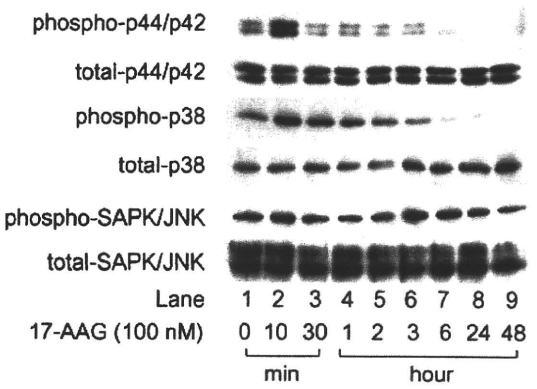

Figure 3. 17-AAG induced phosphorylation of both p44/p42 MAPK and p38 MAPK, but not SAPK/JNK in KP3 pancreatic cancer cells. KP3 cells were treated with 17-AAG (100 nM) for the indicated periods and protein extracts were then harvested and examined by Western blotting using anti-phospho-p44/p42 MAPK, anti-p44/p42 MAPK, anti-phospho-p38 MAPK, anti-p38 MAPK, anti-phospho-SAPK/JNK and anti-SAPK/JNK antibodies.

it is likely that the suppression of pancreatic cancer cell proliferation caused by inhibition of HSP90 is generally correlated with either phosphorylation of EGFR at Ser1046/7 or its desensitization.

HSP90 inhibitors induced activation of p44/p42 MAPK and p38 MAPK in KP3 human pancreatic cancer cells. It has been shown that the inhibition of HSP90 destabilizes a large number of oncogenes that are themselves overexpressed, mutated or otherwise activated during malignant progression (26). HSP90 client proteins include various molecules associated with the initiation and development of cancer, such as the kinases c-Raf1, HER-2, Akt, cdk4 and p53. In the present study, we examined the effect of 17-AAG on activation of kinase cascades, especially the MAP kinase superfamily. We found that 17-AAG induced activation of both p44/p42 MAPK and p38 MAPK in KP3 cells (Fig. 3). On the contrary, 17-AAG had little effect on the activation of SAPK/JNK (Fig. 3). These results led us to further investigate

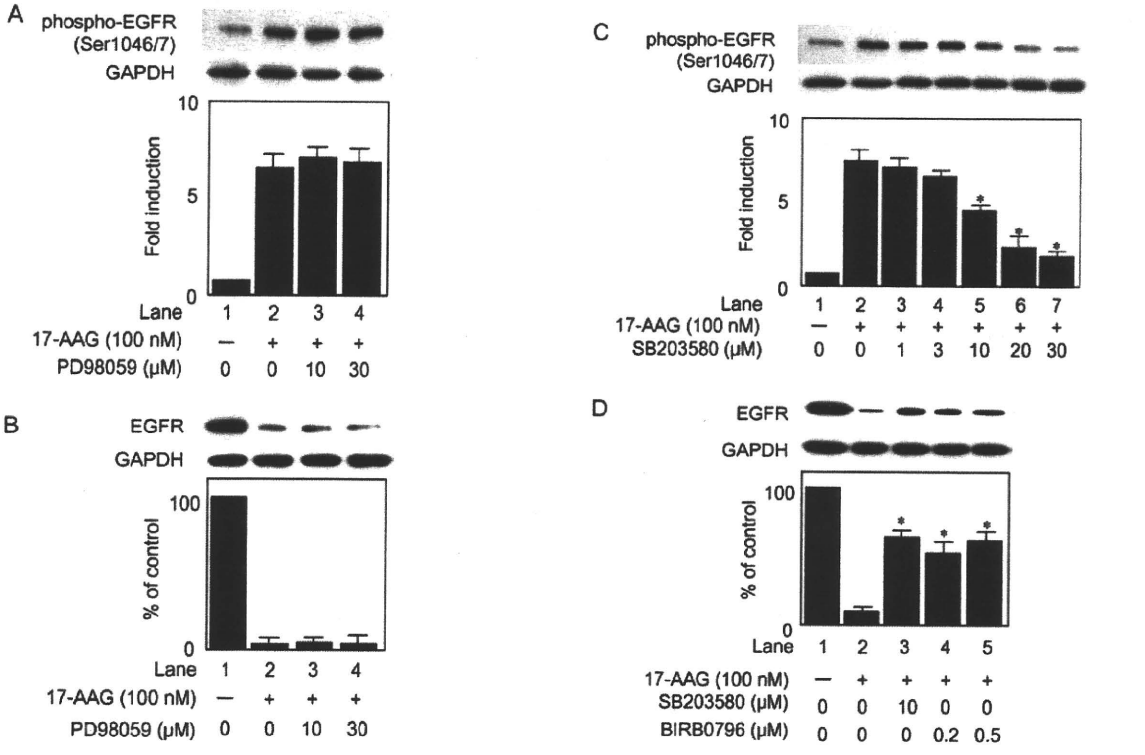

Figure 4. The inhibition of p38 MAPK, but not p44/p42 MAPK suppressed the phosphorylation of EGFR at Ser1046/7 and desensitization of EGFR induced by 17-AAG in KP3 pancreatic cancer cells. (A) KP3 cells were pretreated with PD98059 at the indicated doses for 1 h, followed by treatment with 17-AAG (100 nM) for 1 h. Protein extracts were then harvested and examined by Western blotting using anti-phospho-EGFR at Ser1046/7 and anti-GAPDH antibodies. The lower bar graph shows quantification data for the relative levels of phospho-EGFR at Ser1046/7, after normalization with respect to GAPDH, as determined by densitometry. (B) KP3 cells were pretreated with PD98059 at the indicated doses for 1 h, followed by treatment with 17-AAG (100 nM) for 48 h. Protein extracts were then harvested and examined by Western blotting using anti-EGFR and anti-GAPDH antibodies. The lower bar graph shows quantification data for the relative levels of EGFR, after normalization with respect to GAPDH, as determined by densitometry. (C) KP3 cells were pretreated with SB203580 at the indicated doses for 1 h, followed by treatment with 17-AAG (100 nM) for 1 h. Protein extracts were then harvested and examined by Western blotting using anti-phospho-EGFR at Ser1046/7 and anti-GAPDH antibodies. The lower bar graph shows quantification data for the relative levels of phospho-EGFR at Ser1046/7, after normalization with respect to GAPDH, as determined by densitometry. (D) KP3 cells were pretreated with either SB203580 or BIRB0796, p38 MAPK inhibitors, at the indicated doses for 1 h, followed by treatment with 17-AAG (100 nM) for 48 h. Protein extracts were then harvested and examined by Western blotting using anti-EGFR and anti-GAPDH antibodies. The lower bar graph shows quantification data for the relative levels of EGFR, after normalization with respect to GAPDH, as determined by densitometry. The asterisks indicate significant increase ($^*p<0.05$) as compared to the control (lane 2), respectively.

whether activation of either p44/p42 MAPK or p38 MAPK plays a role in the desensitization of EGFR induced by HSP90 inhibitors in pancreatic cancer cells.

Inhibition of p38 MAPK, but not p44/p42 MAPK suppressed the phosphorylation of EGFR at Ser1046/7. As shown in Fig. 3, 17-AAG induced the activation of p44/p42 MAPK and p38 MAPK in KP3 cells. In addition, HSP90 inhibitors including 17-AAG caused the phosphorylation of EGFR at Ser1046/7 (Figs. 1 and 2). Therefore, it is of interest to examine the effects of MEK1/2 specific inhibitor, PD98059 (27) or p38 MAPK specific inhibitor, SB203580 (28) on the phosphorylation of EGFR at Ser1046/7 and the desensitization of EGFR induced by 17-AAG. As shown in Fig. 4A, the phosphorylation of EGFR at Ser1046/7 induced by 17-AAG was not suppressed even when the cells were pretreated with up to 30 μM of PD98059 (Fig. 4A), a dose of which strongly suppressed the phosphorylation of p44/p42 MAPK induced by 17-AAG (data not shown). Additionally, PD98059 failed to reverse the desensitization of EGFR induced by 17-AAG (Fig. 4B). Therefore, it is unlikely that p44/p42 MAPK is involved in the desensitization of EGFR by HSP90 inhibitors. On the contrary, 17-AAG-induced phosphorylation of EGFR at Ser1046/7 was significantly inhibited by treatment with SB203580 at doses of over 10 μM (Fig. 4C). Moreover, EGFR desensitization induced by 17-AAG was significantly restored when the cells were pretreated with specific inhibitors of p38 MAPK, either SB203580 or BIRB0796 (29) (Fig. 4D). These results strongly suggest that phosphorylation of EGFR at Ser1046/7 was mediated through the p38 MAPK pathway and that the p38 MAPK pathway, at least in part, acts in 17-AAG-induced EGFR desensitization in KP3 pancreatic cancer cells.

Discussion

The benzoquinone ansamycin antibiotic geldanamycin was discovered as a natural product which disrupts HSP90 chaperone activities and its less toxic derivative 17-AAG has been shown to possess strong anti-proliferative and apoptotic activity in cancer cells, whereas 17-AAG has demonstrated potent anti-tumor activity in several human xenograft models, including breast, prostate and colon cancer (30). Therefore, we examined the effect of 17-AAG on anti-proliferative effect, especially focusing on desensitization of EGFR in various kinds of pancreatic cancer cells. Our findings show in pancreatic cancer cells that: i) EGFR is targeted by HSP90 inhibitors; ii) HSP90 inhibitors induce activation of p38 MAPK; iii) the inhibition of HSP90 induces the EGFR phosphorylation at Ser1046/7, a site which is reported to play an important role in its desensitization; and iv) p38 MAPK regulates desensitization of EGFR via its phosphorylation at Ser1046/7. Our present study in pancreatic cancer cells is consistent with our previous report showing that p38 MAPK directs EGFR toward desensitization via its phosphorylation at Ser1046/7 (22), because in the present study we found that HSP90 inhibitors induced p38 MAPK, leading to EGFR phosphorylation at Ser1046/7.

Recent study shows that several HSP90 client proteins have been validated as clinically important therapeutic targets for treatment of cancer, and HSP90 inhibitors are recognized as potentially beneficial anti-cancer agents (31). More than 200 signaling proteins have been found to be regulated by HSP90. For example, BCR-ABL is degraded after HSP90 inhibition and imatinib-resistant BCR-ABL point mutants remain sensitive to HSP90 inhibitors (32). Lung cancers are sometimes driven by mutant HER-2, mutant B-Raf, or mutant or overexpressed c-Met, all of which are also degraded by HSP90 inhibition (33). Moreover, it has been reported that HSP90 plays a unique anti-apoptotic role in small cell lung cancer cells, so that HSP90 inhibition results in substantial cell death in both chemosensitive and chemoresistant cell lines (33). Since many of HSP90-regulated signaling proteins are involved in cancer cell growth, HSP90 inhibitors are recognized as a promising new class of anti-cancer drugs (34). Moreover, HSP90 in human pancreatic cancer is reportedly expressed 6- to 7-fold higher than normal tissues (35). In addition, enhanced EGFR signaling pathway contributes to pancreatic cancer (4). We herein showed that HSP90 inhibitors induced EGFR desensitization in pancreatic cancer cells (Figs. 1 and 2), thus indicating that HSP90 inhibitors might be useful for control of pancreatic cancer.

There is accumulating evidence that activation of p38 MAPK has a suppressive effect on tumorigenesis (36) and that a variety of agents, in addition to specific ligands such as EGF and transforming growth factor α, can induce activation of p38 MAPK and internalization of EGFR into endosomal vesicles. These agents include oxidative stress (37), ultraviolet irradiation (38), gemcitabine (39) and cisplatin (40). We have previously reported that (-)-epigallocatechin gallate (EGCG) caused internalization of EGFR into endosomal vesicles (23). Moreover, we have recently shown that EGCG downregulates EGFR via phosphorylation at Ser1046/7 by p38 MAPK in colon cancer cells (25). In the present study, we investigated the involvement of p38 MAPK in EGFR desensitization induced by HSP90 inhibitors and showed that p38 MAPK activated by HSP90 inhibitors induced desensitization of EGFR via its phosphorylation at Ser1046/7. Based on these findings, it is most likely that p38 MAPK plays a key role in EGFR desensitization.

It has previously been reported that whereas the kinase domain of HER-2 is assembled into a stable complex with HSP90, little or no HSP90 is recovered with EGFR (41). In addition, mutant EGFR is reported to be one of HSP90 clients (14). However, as far as we know, there is no report showing that pancreatic cancer has mutant EGFR. Therefore, our present study provides the first evidence showing that HSP90 inhibitors induced desensitization of wild-type EGFR in pancreatic cancer cells. Our findings may suggest new therapeutic strategies for inhibiting the proliferation of pancreatic cancer that are highly dependent on the function of the EGFR. As mentioned above, gemcitabine is currently considered to be the standard of care for the treatment of advanced pancreatic cancer. Since the potency of combination of gemcitabine with certain other cytotoxic drugs have been investigated in several clinical trials (2), it is of interest to elucidate new combination of gemcitabine and HSP90 inhibitors in human pancreatic cancer. Although our present study elucidated the mechanism underlying EGFR desensitization induced by HSP90 inhibitors, further

investigation is required to clarify how HSP90 inhibitors activate p38 MAPK and how phosphorylation of EGFR at Ser1046/7 induces desensitization of EGFR.

In conclusion, our results strongly suggest that HSP90 inhibitors cause EGFR desensitization in human pancreatic cancer cells and that activation of p38 MAPK induced by HSP90 inhibitors regulates the desensitization of EGFR via its phosphorylation at Ser1046/7.

Acknowledgements

We are very grateful to Ms. Yoko Kawamura for her skillful technical assistance. This study was supported in part by Grant-in-Aid for Scientific Research (20790490 to S.A) from the Ministry of Education, Science, Sports and Culture of Japan.

References

1. Jemal A, Siegel R, Ward E, Murray T, Xu J and Thun MJ: Cancer statistics, 2007. CA Cancer J Clin 57: 43-66, 2007.
2. Sanchez SE and Trevino JG: Current adjuvant and targeted therapies for pancreatic adenocarcinoma. Curr Med Chem 15: 1674-1683, 2008.
3. Zandi R, Larsen AB, Andersen P, Stockhausen MT and Poulsen HS: Mechanisms for oncogenic activation of the epidermal growth factor receptor. Cell Signal 19: 2013-2023, 2007.
4. Papageorgio C and Perry MC: Epidermal growth factor receptor-targeted therapy for pancreatic cancer. Cancer Invest 25: 647-657, 2007.
5. Velu TJ, Beguinot L, Vass WC, *et al*: Epidermal-growth-factor-dependent transformation by a human EGF receptor proto-oncogene. Science 238: 1408-1410, 1987.
6. Xiong HQ and Abbruzzese JL: Epidermal growth factor receptor-targeted therapy for pancreatic cancer. Semin Oncol 29: 31-37, 2002.
7. Baselga J: The EGFR as a target for anticancer therapy - focus on cetuximab. Eur J Cancer 37 (Suppl. 4): S16-S22, 2001.
8. Milano G, Spano JP and Leyland-Jones B: EGFR-targeting drugs in combination with cytotoxic agents: from bench to bedside, a contrasted reality. Br J Cancer 99: 1-5, 2008.
9. Chiosis G: Targeting chaperones in transformed systems, a focus on Hsp90 and cancer. Expert Opin Ther Targets 10: 37-50, 2006.
10. Prodromou C and Pearl LH: Structure and functional relationships of Hsp90. Curr Cancer Drug Targets 3: 301-323, 2003.
11. Smith V, Hobbs S, Court W, Eccles S, Workman P and Kelland LR: ErbB2 overexpression in an ovarian cancer cell line confers sensitivity to the HSP90 inhibitor geldanamycin. Anticancer Res 22: 1993-1999, 2002.
12. Zhang H and Burrows F: Targeting multiple signal transduction pathways through inhibition of Hsp90. J Mol Med 82: 488-499, 2004.
13. Mabjeesh NJ, Post DE, Willard MT, *et al*: Geldanamycin induces degradation of hypoxia-inducible factor 1alpha protein via the proteosome pathway in prostate cancer cells. Cancer Res 62: 2478-2482, 2002.
14. Shimamura T, Lowell AM, Engelman JA and Shapiro GI: Epidermal growth factor receptors harboring kinase domain mutations associate with the heat shock protein 90 chaperone and are destabilized following exposure to geldanamycins. Cancer Res 65: 6401-6408, 2005.
15. Panaretou B, Siligardi G, Meyer P, *et al*: Activation of the ATPase activity of hsp90 by the stress-regulated cochaperone aha1. Mol Cell 10: 1307-1318, 2002.
16. Banerji U, Walton M, Raynaud F, *et al*: Pharmacokinetic-pharmacodynamic relationships for the heat shock protein 90 molecular chaperone inhibitor 17-allylamino, 17-demethoxygeldanamycin in human ovarian cancer xenograft models. Clin Cancer Res 11: 7023-7032, 2005.
17. Arteaga CL: Epidermal growth factor receptor dependence in human tumors: more than just expression? Oncologist 7 (Suppl. 4): 31-39, 2002.
18. Massie C and Mills IG: The developing role of receptors and adaptors. Nat Rev Cancer 6: 403-409, 2006.
19. Countaway JL, McQuilkin P, Girones N and Davis RJ: Multisite phosphorylation of the epidermal growth factor receptor. Use of site-directed mutagenesis to examine the role of serine/threonine phosphorylation. J Biol Chem 265: 3407-3416, 1990.
20. Countaway JL, Nairn AC and Davis RJ: Mechanism of desensitization of the epidermal growth factor receptor protein-tyrosine kinase. J Biol Chem 267: 1129-1140, 1992.
21. Theroux SJ, Stanley K, Campbell DA and Davis RJ: Mutational removal of the major site of serine phosphorylation of the epidermal growth factor receptor causes potentiation of signal transduction: role of receptor down-regulation. Mol Endocrinol 6: 1849-1857, 1992.
22. Adachi S, Natsume H, Yamauchi J, *et al*: p38 MAP kinase controls EGF receptor downregulation via phosphorylation at Ser1046/1047. Cancer Lett 277: 108-113, 2009.
23. Adachi S, Nagao T, To S, *et al*: (-)-Epigallocatechin gallate causes internalization of the epidermal growth factor receptor in human colon cancer cells. Carcinogenesis 29: 1986-1993, 2008.
24. Adachi S, Nagao T, Ingolfsson HI, *et al*: The inhibitory effect of (-)-epigallocatechin gallate on activation of the epidermal growth factor receptor is associated with altered lipid order in HT29 colon cancer cells. Cancer Res 67: 6493-6501, 2007.
25. Adachi S, Shimizu M, Shirakami Y, *et al*: (-)-Epigallocatechin gallate downregulates EGF receptor via phosphorylation at Ser1046/1047 by p38 MAP kinase in colon cancer cells. Carcinogenesis 30: 1544-1552, 2009.
26. Workman P: Overview: translating Hsp90 biology into Hsp90 drugs. Curr Cancer Drug Targets 3: 297-300, 2003.
27. Alessi DR, Cuenda A, Cohen P, Dudley DT and Saltiel AR: PD 098059 is a specific inhibitor of the activation of mitogen-activated protein kinase kinase in vitro and in vivo. J Biol Chem 270: 27489-27494, 1995.
28. Cuenda A, Rouse J, Doza YN, *et al*: SB 203580 is a specific inhibitor of a MAP kinase homologue which is stimulated by cellular stresses and interleukin-1. FEBS Lett 364: 229-233, 1995.
29. Bain J, Plater L, Elliott M, *et al*: The selectivity of protein kinase inhibitors: a further update. Biochem J 408: 297-315, 2005.
30. Stravopodis DJ, Margaritis LH and Voutsinas GE: Drug-mediated targeted disruption of multiple protein activities through functional inhibition of the Hsp90 chaperone complex. Curr Med Chem 14: 3122-3138, 2007.
31. Soo ET, Yip GW, Lwin ZM, Kumar SD and Bay BH: Heat shock proteins as novel therapeutic targets in cancer. In Vivo 22: 311-315, 2008.
32. Gorre ME, Ellwood-Yen K, Chiosis G, Rosen N and Sawyers CL: BCR-ABL point mutants isolated from patients with imatinib mesylate-resistant chronic myeloid leukemia remain sensitive to inhibitors of the BCR-ABL chaperone heat shock protein 90. Blood 100: 3041-3044, 2002.
33. Shimamura T and Shapiro GI: Heat shock protein 90 inhibition in lung cancer. J Thorac Oncol 3: S152-S159, 2008.
34. Sharp S and Workman P: Inhibitors of the HSP90 molecular chaperone: current status. Adv Cancer Res 95: 323-348, 2006.
35. Ogata M, Naito Z, Tanaka S, Moriyama Y and Asano G: Over-expression and localization of heat shock proteins mRNA in pancreatic carcinoma. J Nippon Med Sch 67: 177-185, 2000.
36. Kennedy NJ, Cellurale C and Davis RJ: A radical role for p38 MAPK in tumor initiation. Cancer Cell 11: 101-103, 2007.
37. Khan EM, Heidinger JM, Levy M, Lisanti MP, Ravid T and Goldkorn T: Epidermal growth factor receptor exposed to oxidative stress undergoes Src- and caveolin-1-dependent perinuclear trafficking. J Biol Chem 281: 14486-14493, 2006.
38. Oksvold MP, Huitfeldt HS, Ostvold AC and Skarpen E: UV induces tyrosine kinase-independent internalisation and endosome arrest of the EGF receptor. J Cell Sci 115: 793-803, 2002.
39. Feng FY, Varambally S, Tomlins SA, *et al*: Role of epidermal growth factor receptor degradation in gemcitabine-mediated cytotoxicity. Oncogene 26: 3431-3439, 2007.
40. Winograd-Katz SE and Levitzki A: Cisplatin induces PKB/-Akt activation and p38(MAPK) phosphorylation of the EGF receptor. Oncogene 25: 7381-7390, 2006.
41. Xu W, Mimnaugh E, Rosser MF, *et al*: Sensitivity of mature Erbb2 to geldanamycin is conferred by its kinase domain and is mediated by the chaperone protein Hsp90. J Biol Chem 276: 3702-3708, 2001.

Role of Acid Sphingomyelinase of Kupffer Cells in Cholestatic Liver Injury in Mice

Yosuke Osawa,[1,2] Ekihiro Seki,[3] Masayuki Adachi,[3] Atsushi Suetsugu,[2] Hiroyasu Ito,[1] Hisataka Moriwaki,[2] Mitsuru Seishima,[1] and Masahito Nagaki[2]

Kupffer cells, resident tissue macrophages of the liver, play a key role in the regulation of hepatic inflammation, hepatocyte death, and fibrosis that characterize liver diseases. However, it is controversial whether Kupffer cells promote or protect from liver injury. To explore this issue we examined the role of Kupffer cells in liver injury, cell death, regeneration, and fibrosis on cholestatic liver injury in C57BL/6 mice using a model of partial bile duct ligation (BDL), in which animals do not die and the effects of BDL can be compared between injured ligated lobes and nonligated lobes. In cholestatic liver injury, the remaining viable cells represented tolerance for tumor necrosis factor alpha (TNF-α)-induced hepatocyte apoptosis and regenerative features along with AKT activation. Inhibition of AKT by adenovirus expressing dominant-negative AKT abolished the survival and regenerative properties in hepatocytes. Moreover, Kupffer cell depletion by alendronate liposomes increased hepatocyte damage and the sensitivity of TNF-α-induced hepatocyte apoptosis in ligated lobes. Kupffer cell depletion decreased hepatocyte regeneration and liver fibrosis with reduced AKT activation. To investigate the impact of acid sphingomyelinase (ASMase) in Kupffer cells, we generated chimeric mice that contained ASMase-deficient Kupffer cells and -sufficient hepatocytes using a combination of Kupffer cell depletion, irradiation, and the transplantation of ASMase-deficient bone marrow cells. In these mice, AKT activation, the tolerance for TNF-α-induced apoptosis, and the regenerative responses were attenuated in hepatocytes after BDL. *Conclusion:* Kupffer cells have a protective role for hepatocyte damage and promote cell survival, liver regeneration, and fibrosis in cholestatic liver disease. Kupffer cell-derived ASMase is crucial for AKT activation of hepatocytes that is required for the survival and regenerative responses. (HEPATOLOGY 2010;51:237-245.)

Chronic liver disease is associated with inflammatory cell infiltration, cytokine production, and liver cell death. Persistent hepatocyte death impairs hepatocyte regeneration accompanied with excessive production of extracellular matrix proteins causing liver fibrosis. Kupffer cells, resident tissue macrophages of the liver, function as both a promoter and a protector against liver injury. Lipopolysaccharide activates Kupffer cells and induces liver injury and inhibition of Kupffer cells prevents liver injury.[1] In addition, inhibition of Kupffer cell activation prevents liver injury induced by melphalan[2] and fumonisin B1.[3] In contrast, reduced Kupffer cell activity augments some kinds of liver injuries, such as hepatectomy- or acetaminophen-induced liver injury.[4,5] Activated Kupffer cells release various types of inflammatory cytokines and growth factors,[6] and these mediators are thought to regulate liver injury and regeneration. Especially, tumor necrosis factor alpha (TNF-α) from activated Kupffer cells plays a major role in the pathogenesis of various liver injuries.[7,8] Cholestasis is associated with many liver diseases. Bile duct ligation (BDL) causes hepatocyte damage, hepatic stellate cell (HSC) activation, and liver fibrosis accompanied by Kupffer cell activation leading to the production of a variety of cytokines and chemokines that are involved in liver damage and fibrosis.[9-11] Because these features are similar to human cholestatic diseases,

Abbreviations: α-SMA, alpha smooth muscle actin; Ale-lip, liposome-encapsulated alendronate; ASMase, acid sphingomyelinase; BDL, bile duct ligation; DN, dominant negative; GalN, D-galactosamine; GSK, glycogen synthase kinase; HSC, hepatic stellate cell; PBDL, partial BDL; TNF-α, tumor necrosis factor alpha; TUNEL, terminal deoxynucleotidyl transferase nick end-labeling.

From the [1]Department of Informative Clinical Medicine, Gifu University Graduate School of Medicine, Gifu, Japan; [2]Department of Gastroenterology, Gifu University Graduate School of Medicine, Gifu, Japan; [3]Department of Medicine, University of California San Diego, School of Medicine, La Jolla, CA, USA.

Received April 23, 2009; accepted August 23, 2009.

Supported by Grant-in-Aid from the Ministry of Education, Culture, Sports, Science, and Technology of Japan (19790478) (21790657) (both to Y.O.) and by a Liver Scholar Award from the AASLD/ALF (to E.S.).

Address reprint requests to: Yosuke Osawa M.D. PhD., Department of Informative Clinical Medicine, Gifu University Graduate School of Medicine, 1-1 Yanagido Gifu, 501-1194, Japan. E-mail:osawa-gif@umin.ac.jp; fax: 81-58-230-6431.

Published online in Wiley InterScience (www.interscience.wiley.com).

DOI 10.1002/hep.23262

Potential conflict of interest: Nothing to report.

Additional Supporting Information may be found in the online version of this article.

common BDL has been used as an animal model of chronic liver disease. However, in this model, common bile duct ligation causes total bile acid reflux to damage whole liver, and the animals show high mortality due to liver failure. We have previously established a partial BDL (PBDL) model, in which animals showed a typical liver injury only in the BDL lobes but no damage in the nonligated lobes with viable liver functions. In this study we examined the role of Kupffer cells in chronic liver injury using the PBDL model.

Acid sphingomyelinase (ASMase) hydrolyses sphingomyelin into ceramide and phosphorylcholine and is involved in various cell functions. Ceramide has been identified as a bioactive mediator of various cellular functions.[12] In addition, roles for sphingomyelin and ceramide in membrane lipid rafts have been reported,[13] which is related with transmitting signals across the plasma membrane. In macrophages, ASMase contributes to cytokine and chemokine release. Its inhibitor, sphingomyeline difluoromethylene analogue-7 (SMA-7), suppressed lipopolysaccharide-induced releases of TNF-α, interleukin (IL)-1β, and IL-6 from macrophages, and it reduces the severity of inflammatory bowel disease induced by dextran sodium sulfate.[14] In contrast, production of macrophage inflammatory protein-1α and -2 is increased in ASMase-deficient macrophages.[15] In addition, ASMase-deficient macrophage is impaired in killing bacteria.[16] Thus, ASMase contributes to various immunoresponses. In liver damage, although deficiency of ASMase leads to resistance to hepatocyte cell death induced by TNF-α,[17,18] the role of ASMase in Kupffer cells remains unclear.

In this study we assessed the roles of Kupffer cells and ASMase during chronic liver injury using PBDL mice. We found that Kupffer cells reduce liver damage, and induce hepatocyte survival and regeneration, and fibrosis. The protective and regenerative effects require AKT in hepatocytes by way of ASMase in Kupffer cells.

Materials and Methods

Animals and PBDL. ASMase knockout mice (ASMase$^{-/-}$) (C57Bl/6 background)[18] were bred for studies. Eight-week-old male wildtype C57Bl/6J mice were obtained from Japan SLC (Japan). The left hepatic duct was ligated for PBDL as reported.[19] The animals were fasted for 12 hours before sacrifice at 10 days after the surgery. As necessary, hepatocyte apoptosis was induced by mouse TNF-α (R&D Systems, Minneapolis, MN) (0.5 μg/mouse intravenously) with D-galactosamine (GalN) (Nacalai Tesque, Japan) (20 mg/mouse intraperitoneally) 10 days after the PBDL[20] and the animals were killed 6 hours after TNF-α administration. All procedures were approved by the Institutional Animal Care Committee of Gifu University.

Depletion of Kupffer Cells. Alendronate was reported to deplete Kupffer cells.[1] A single injection of liposome-encapsulated alendronate (Ale-lip) depleted F4/80-positive cells in the liver at 2-3 days after injection and the cells started to restore at 6 days (Supporting Fig. 1A). Ale-lip had no effect on hepatocytes with hematoxylin and eosin (H&E) (Supporting Fig. 1B) and alanine transaminase (ALT) (data not shown). The vitamin A autofluorescence and desmin-positive cells, characteristic features of HSCs, were not decreased by Ale-lip (Supporting Fig. 1CD). Ale-lip was injected to the operated mice 3 times at 1 day before surgery and 3 and 6 days after the surgery. Phosphate-buffered saline (PBS) encapsulated liposomes (PBS-lip) were used for control.

Bone Marrow Transplantation. Bone marrow transplantation was performed as reported.[11] The wildtype mice received Ale-lip injection twice at 1 and 4 days prior to lethal irradiation (11 Gy). Total bone marrow cells were collected from wildtype or ASMase$^{-/-}$ mice and injected to the irradiated recipient mice (10^7 cells). PBDL was performed 10 weeks after the transplantation.

Other Experimental Procedures. Other experimental procedures are described in the Supporting experimental procedures. These include preparation of liposome-encapsulated alendronate, adenovirus infection, histological analysis, western blot, quantitative real-time reverse-transcription polymerase chain reaction (RT-PCR), hydroxyproline measurement, and statistical analysis.

Results

Kupffer Cell Depletion Increases Hepatocellular Damage Induced by BDL. To examine the effect of Kupffer cell depletion on chronic liver damage induced by BDL, we initially injected Ale-lip three times to mice operated on with common BDL. Although the treatment with Ale-lip alone did not induce liver injury, the mortality of mice treated with common BDL and Ale-lip was extremely high; 40% 10 days after the surgery. In our established model, PBDL showed liver injury and fibrosis only in BDL lobes, which improved the survival rate up to 100% in Ale-lip-treated mice. Therefore, we decided to use PBDL for this study. In BDL lobes, F4/80-positive cells were increased. The Ale-lip treatment succeeded in deleting F4/80-positive cells (Fig. 1A). Thus, Ale-lip injection can be utilized as a new tool for Kupffer cell depletion. Inflammatory cytokines mainly produced from Kupffer cells were up-regulated in BDL lobes, whereas the

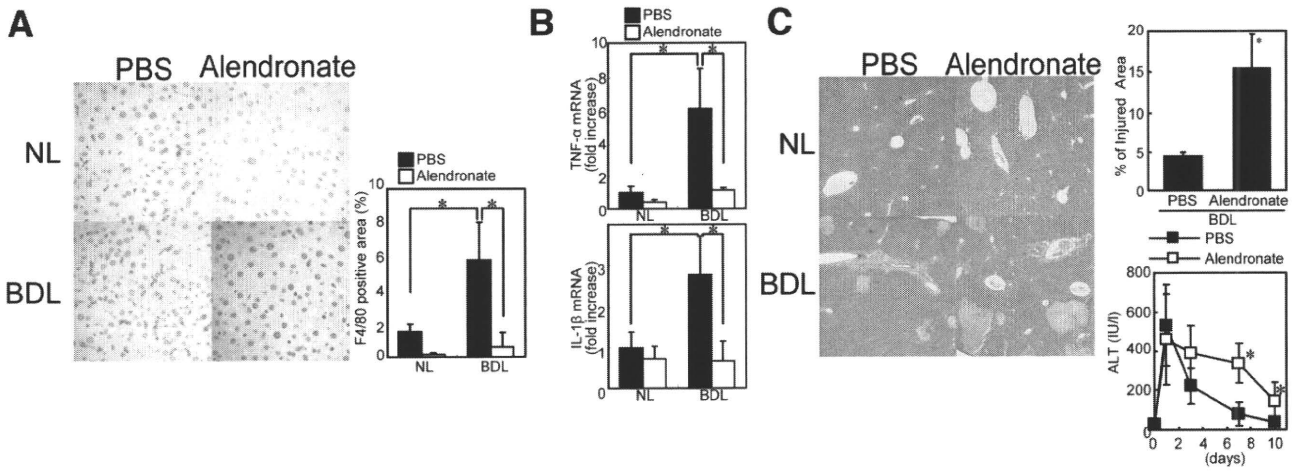

Fig. 1. Depletion of Kupffer cells increased liver injury after BDL. Wildtype mice were subjected to PBDL and treated with Ale-lip or PBS-lip. The animals were killed 10 days after the surgery. (A) Expression of F4/80 in the nonligated (NL) right (upper panel) and BDL left (lower panel) lobes was examined by immunohistochemistry. (Original magnification ×400; graph, right panel.) (B) Hepatic mRNA levels of TNF-α and IL-1β were determined by quantitative real-time RT-PCR. (C) The injured lesion in the ligated left lobes was assessed by H&E staining. (Original magnification ×40; graph, right upper panel.) Serum ALT levels were compared on the indicated time periods. Data are means ± SD from at least four independent experiments. *$P < 0.05$ using Student's t test.

Ale-lip treatment markedly inhibited the production of TNF-α and IL-1β (Fig. 1B). Kupffer cell-depleted mice showed an increase of injured lesion in BDL lobes and serum ALT level after the surgery (Fig. 1C). Interestingly, 24 hours after common BDL (Supporting Fig. 2) as well as PBDL (Fig. 1C), there were no significant differences in histological liver injury and elevated ALT activities between control and Kupffer cell-depleted mice. These findings indicate that Kupffer cells were not involved in the early stage of liver damage that occurs by BDL, but in the late stage.

Kupffer Cells Mediate Survival and Regeneration of Hepatocyte by BDL. As previously reported,[20] treatment with TNF-α plus GalN strongly induced hepatocyte destruction and massive hemorrhage with apoptotic cells in nonligated lobes of PBDL animals, whereas hemorrhagic damage and hepatocyte apoptosis were blunted in BDL lobes (Supporting Fig. 3A-C). Kupffer cell depletion itself did not induce hepatocyte apoptosis (Supporting Fig. 3D). In Kupffer cell-depleted livers, GalN plus TNF-α treatment induced hemorrhagic liver damage and hepatocyte apoptosis with the cleavage of poly (ADP-ribose) polymerase (PARP), which is the downstream target of caspase-3, both in nonligated and BDL lobes (Fig. 2A-C).

In the BDL lobes, proliferation cell nuclear antigen (PCNA) or Ki67-positive hepatocytes were increased with up-regulation of cyclin E expression (Fig. 2D-F), indicating that BDL induces hepatocyte regeneration. In Kupffer cell-depleted livers the expressions of PCNA, Ki67, and cyclin E were decreased (Fig. 2D-F). Thus, Kupffer cells are important for survival and regeneration of hepatocytes after BDL.

Kupffer Cells Are Required for Liver Fibrosis. Fibrosis was induced in BDL lobes as demonstrated by Sirius red staining, hydroxyproline content, expression of α-smooth muscle actin (α-SMA) and desmin, and messenger RNA (mRNA) expression of collagen-α1(I) and transforming growth factor (TGF)-β1 (Fig. 3). Kupffer cell-depleted mice showed reduced fibrosis in BDL lobes (Fig. 3). The number and the activation of HSCs were decreased by Kupffer cell depletion as assessed by desmin and α-SMA expression, respectively. These results suggest that the decrease in the fibrogenic response by Kupffer cell depletion is due to a lack of signal from Kupffer cells to activate and proliferate HSCs.

ASMase Deficiency in Kupffer Cells Diminishes the BDL-Induced Survival and Proliferative Effect. To further elucidate the mechanisms by which Kupffer cells contribute to BDL-mediated functional changes in liver injury, survival of hepatocyte, regeneration, and fibrosis, we focused on ASMase. The protein level of ASMase (Supporting Fig. 4) and ceramides (Supporting Table 1), the metabolite of ASMase, were increased in BDL lobes compared with those in nonligated lobes, suggesting the contribution of ASMase in the liver. To explore the involvement of ASMase in bone marrow-derived cells we generated ASMase-chimeric mice using a combination of alendronate-induced Kupffer cell depletion, irradiation, and bone marrow transplantation. To confirm the substitution of Kupffer cells in chimeric mice we initially generated the mice transplanted with bone marrow isolated

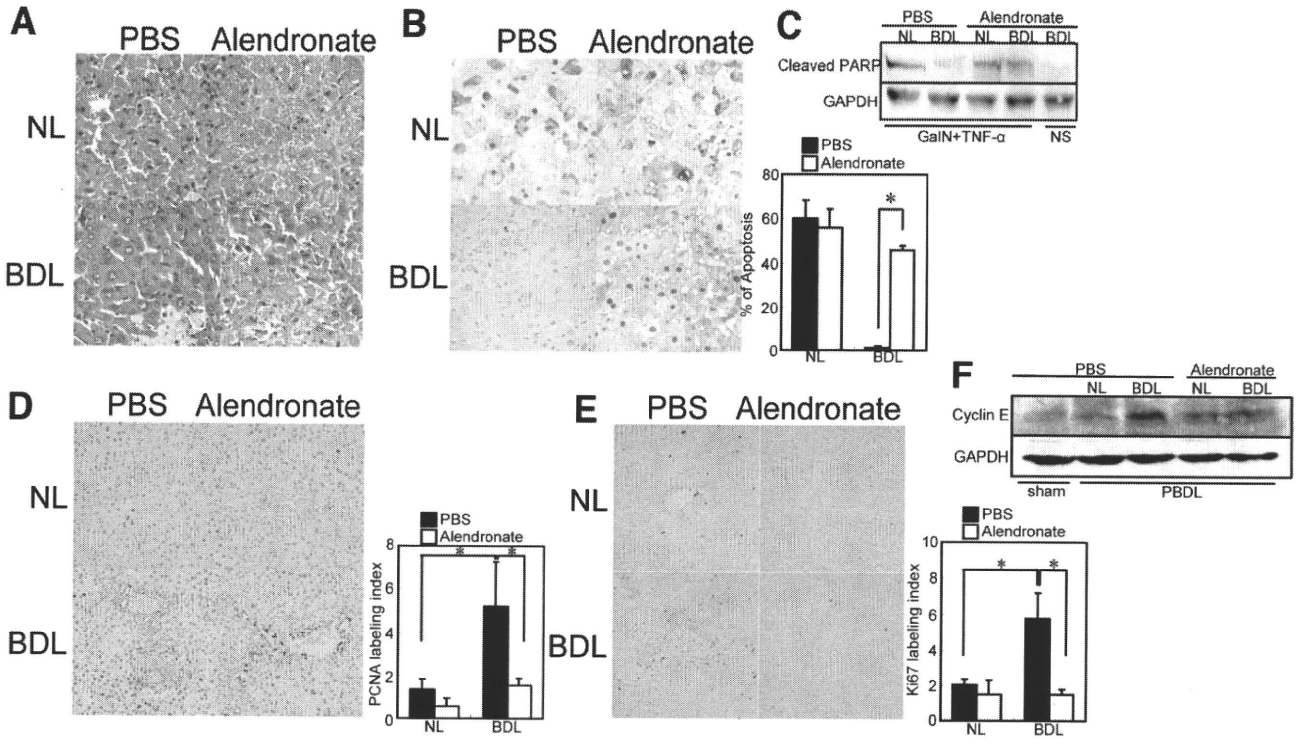

Fig. 2. Depletion of Kupffer cells abolished the survival effect of BDL and decreased hepatocyte regeneration after BDL. Wildtype mice were subjected to PBDL and treated with Ale-lip or PBS-lip. The animals were administered with (A-C) or without (D-F) GalN plus TNF-α (6 hours) on 10 days after the surgery. (A) Liver sections from the nonligated (NL) right (upper panel) and BDL left (lower panel) lobes were stained with H&E. (B) Apoptotic nuclei were identified using TUNEL staining. (Original magnification ×400; graph, right panel.) Expression of PCNA (D) and Ki67 (E) in the NL right (upper panel) and the BDL left (lower panel) lobes were examined by immunohistochemistry. (Original magnification ×200.) PCNA and Ki67 indexes were compared (right panel). Data are means ± SD from at least four independent experiments. *$P < 0.05$ using Student's t test. (C,F) The protein extracts from the NL and BDL lobes were subjected to sodium dodecyl sulfate-polyacrylamide gel electrophoresis (SDS-PAGE) and immunoblotting was performed with anti-PARP, cyclin E, and GAPDH antibodies. The results shown are representative of at least three independent experiments. NS, normal saline.

from β-actin promoter-driven green fluorescent protein (GFP)-transgenic mice. In the GFP-chimeric mouse liver all F4/80-positive cells were GFP-positive (Supporting Fig. 5A), suggesting that this protocol achieved full reconstitution of Kupffer cells to bone marrow-derived cells. The chimeric mice containing ASMase$^{-/-}$ bone marrow cells showed an increase of F4/80-positive cells, and TNF-α and IL-1β production after BDL, which were comparable to ASMase$^{+/+}$ bone marrow-transplanted mice (Supporting Fig. 5BC).

ASMase$^{-/-}$ bone marrow-transplanted mice showed an increase of liver injury in BDL lobes at the same degree as ASMase$^{+/+}$ bone marrow-transplanted mice (Fig. 4), suggesting that ASMase of Kupffer cell is not implicated in the liver injury. Hemorrhagic liver damage and apoptosis with PARP cleavage by GalN plus TNF-α were observed in BDL lobes of ASMase$^{-/-}$ bone marrow-transplanted mice but not in that of ASMase$^{+/+}$ bone marrow-transplanted mice (Fig. 5A-C). An increase of PCNA or Ki67-positive cells with cyclin E expression were blunted in BDL lobes of ASMase$^{-/-}$ bone marrow-transplanted mice (Fig. 5D-F). These results suggest that ASMase in Kupffer cells contribute to the protection against apoptosis and regeneration in BDL lobes. However, there was no difference between ASMase$^{-/-}$ bone marrow and ASMase$^{+/+}$ bone marrow-transplanted mice in mRNA expression of fibrogenic markers, Sirius red staining, and hydroxyproline content (Fig. 6). Thus, ASMase of Kupffer cell was not associated with liver fibrosis.

AKT Activation of Hepatocytes Is Required for Survival and Regeneration in BDL Lobes. Our previous study demonstrated that AKT was up-regulated in BDL lobes and was involved in hepatocyte survival from TNF-α-induced cell death.[20] In BDL lobes, phosphorylated-AKT and its downstream target, phosphorylated-glycogen synthase kinase (GSK)3β were increased (Supporting Fig. 6A). Immunohistochemical analysis identified that AKT in hepatocytes was phosphorylated (Supporting Fig. 6B). The AKT activation in BDL lobes was abrogated by the infection of Ad5 dominant negative (DN)-AKT (Supporting Fig. 6C). The inhibition of AKT abolished the survival effect (Supporting Fig. 6D) as re-

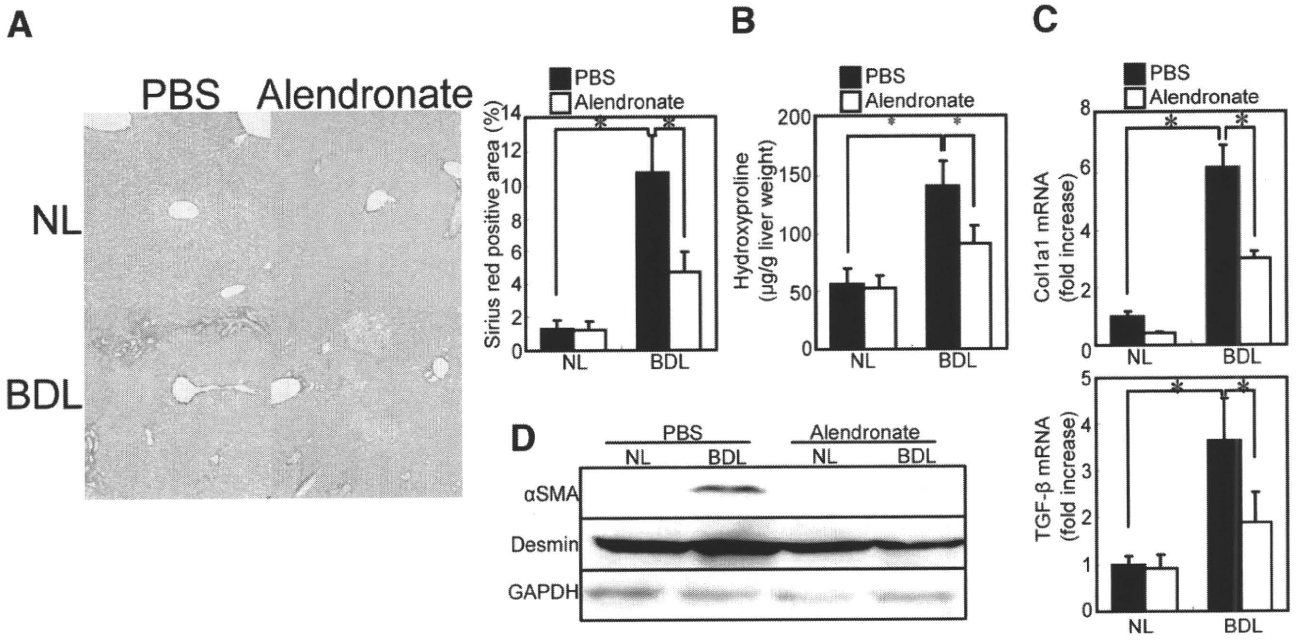

Fig. 3. Depletion of Kupffer cells reduced liver fibrosis after BDL. Wildtype mice were operated on with PBDL and treated with Ale-lip or PBS-lip. The animals were killed 10 days after the surgery. (A,B) Collagen deposition was assessed by Sirius red staining (original magnification ×100; graph, right panel) and measurement of hydroxyproline content. (C) mRNA levels of collagen α1(I) (col1α1) and TGF-β1 (TGF-β) in the livers were determined by quantitative real-time RT-PCR. Data are means ± SD from at least four independent experiments. *$P < 0.05$ using Student's t test. (D) The protein extracts from the livers were subjected to SDS-PAGE and immunoblotting was performed with anti-α-SMA, desmin, and GAPDH antibodies. The results shown are representative of at least three independent experiments.

ported,[20] and eliminated the induction of Ki67-positive cells and cyclin E (Fig. 7A,B) induced by BDL. These findings suggest that AKT activation in hepatocytes is essential for hepatocyte survival and regeneration observed in BDL lobes. In Kupffer cell-depleted mice (Fig. 7C) or ASMase$^{-/-}$ bone marrow-transplanted mice (Fig. 7D), the phosphorylation of AKT and GSK3β by BDL was inhibited. Thus, Kupffer cells and their ASMase are required for AKT-mediated survival and regeneration induced by BDL. Mcl-1 induction, which is a Bcl-2 family member and was regulated by AKT in hepatocytes (Supporting Fig. 6C,E),[21] was diminished in Kupffer cell-depleted mice or ASMase$^{-/-}$ bone marrow-transplanted mice, whereas Bcl-XL or Bfl-1 were not affected. These results suggest that survival may be mediated by Mcl-1 at the downstream of AKT.

Discussion

The present study specifically addressed the role of Kupffer cells and of ASMase in the cholestatic liver injury. Our results demonstrate that depletion of Kupffer cells

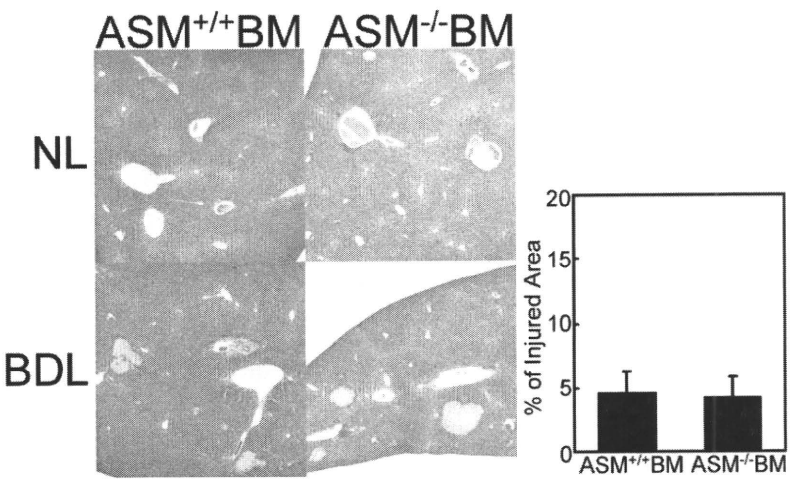

Fig. 4. Reconstitution of Kupffer cells with ASMase knockout cells did not affect on the liver injury induced by BDL. The ASMase$^{+/+}$ bone marrow or ASMase$^{-/-}$ bone marrow-transplanted mice were subjected to PBDL and killed 10 days after the surgery. Measurement of injured lesion in the BDL lobes was assessed with H&E. (Original magnification ×40; graph, right panel.) Data are means ± SD from at least four independent experiments.

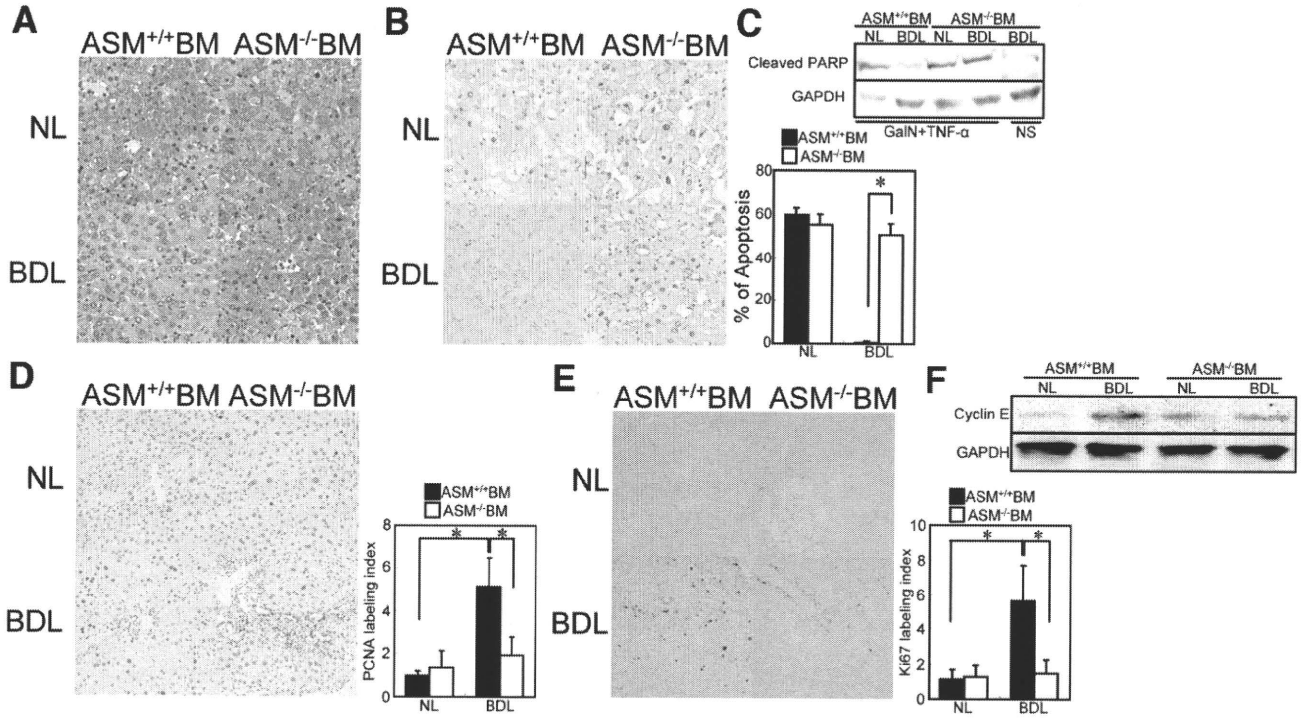

Fig. 5. Reconstitution of Kupffer cells to ASMase knockout cells abrogated the survival effect of BDL and decreased hepatocyte regeneration after BDL. The ASMase$^{+/+}$ bone marrow or ASMase$^{-/-}$ bone marrow-transplanted mice were operated on with PBDL and treated with (A-C) or without (D-F) GalN plus TNF-α treatment (6 hours) 10 days after the surgery. (A) Liver sections were stained with H&E. (B) Apoptotic nuclei were identified using TUNEL staining. (Original magnification $\times$400; graph, right panel.) Expression of PCNA (D) and Ki67 (E) in the nonligated (NL) right (upper panel) and the BDL left (lower panel) lobes was examined by immunohistochemistry. (Original magnification $\times$200.) PCNA and Ki67 indexes were compared (right panel). Data are means $\pm$ SD from at least four independent experiments. *$P < 0.05$ using Student's t test. (C,F) The protein extracts from the NL and BDL lobes were subjected to SDS-PAGE and immunoblotting was performed with anti-PARP, anti-cyclin E, and GAPDH antibodies. The results shown are representative of at least four independent experiments. NS, normal saline.

increased liver injury and susceptibility to TNF-α-induced hepatocyte apoptosis, and decreased hepatocyte regeneration and liver fibrosis with reduced AKT activation. Kupffer cell-derived ASMase was crucial for the AKT activation. The results raise novel therapeutic possibilities for treating liver injury.

After BDL, hepatocytes are exposed to elevated concentrations of bile acid, and hydrophobic bile acids lead to hepatocyte cell death[22] through various factors such as reactive oxygen species (ROS) generation from mitochondria[23] and activation of Fas signaling in a ligand-independent manner by altering cellular trafficking of Fas.[24] Indeed, expression of 4-hydroxy-2-nonenal (HNE), which is produced by lipid peroxidation, was increased on 1 day after the surgery of BDL (data not shown). Because Kupffer cell depletion did not increase the initial liver damage by BDL (1 day after the surgery), it is likely that this damage is induced by a direct toxic effect of bile acid rather than subsequent immune responses because Kupffer cells are not activated in this early stage. The initial hepatocyte cell death stimulates subsequent inflammatory responses leading to further liver injury and fibrosis.[25,26] In BDL liver, the engulfment of apoptotic or necrotic body in Kupffer cells is observed,[27] which leads to production of cytokines including TNF-α and TGF-β.[9] Either a promotive[9] or protective[10] effect of Kupffer cells on BDL-induced liver injury have been reported. In the present study, alendronate treatment, which depleted Kupffer cells in the livers, increased liver injury and reduced fibrosis 10 days after BDL, suggesting that Kupffer cells have a protective effect on the subsequent damage of hepatocytes and a promotive effect on fibrosis in the late stage. The increase of liver injury is probably explained by the diminished Kupffer cell functions, including the phagocytosis of injured tissue and the production of protective factors for hepatocytes. The reduced fibrosis is most likely due to decreased fibrogenic cytokines from Kupffer cells. Cytokines including TGF-β and TGF-α are released from Kupffer cells,[28] and HSCs are stimulated to induce collagen I α1 transcription by TGF-β.[29]

In the liver chronically injured by BDL, hepatocytes represented the survival and regenerative properties, and AKT was a critical factor for the survival and regeneration of the remaining viable hepatocytes. Indeed, overexpression of constitutive active-AKT led hepatocytes to be re-

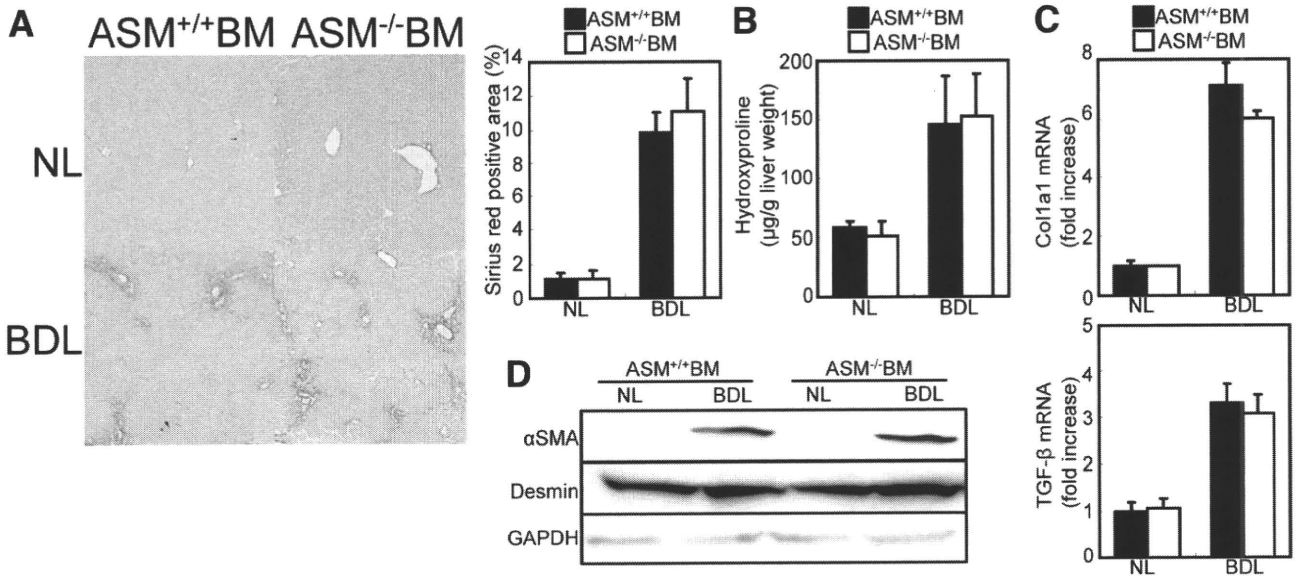

Fig. 6. Reconstitution of Kupffer cells to ASMase knockout cells did not affect the liver fibrosis induced by BDL. The ASMase$^{+/+}$ bone marrow or ASMase$^{-/-}$ bone marrow-transplanted mice were operated on with PBDL and killed 10 days after the surgery. (A,B) Collagen deposition was assessed by Sirius red staining (A) (original magnification ×100; graph, right panel) and measurement of hydroxyproline content (B). (C) mRNA levels of collagen α1(I) (col1a1) and TGF-β1 (TGF-β) in the livers were determined by quantitative real-time RT-PCR. Data are means ± SD from at least five independent experiments. (D) The protein extracts from the livers were subjected to SDS-PAGE and immunoblotting was performed with anti-α-SMA, desmin, and GAPDH antibodies. The results shown are representative of at least three independent experiments.

sistant against TNF-α-induced apoptosis in primary cultured hepatocytes (data not shown) and promoted hepatocyte proliferation by cyclin E.[30] Because depletion of Kupffer cells diminished the survival and regeneration of hepatocytes with reduced AKT activation, Kupffer cells could produce factors that activate AKT in hepatocytes. In our study, the survival and regenerative effects of AKT activation were abrogated in ASMase$^{-/-}$ bone marrow-transplanted mice, suggesting that ASMase in Kupffer cells requires the production of unknown factors that lead to the activation of AKT in hepatocytes. mRNA expression of TNF-α, IL-1β, and IL-6 in ASMase$^{-/-}$ bone marrow-transplanted mice were similar to those in ASMase$^{+/+}$ bone marrow-transplanted mice (Supporting Fig. 5 and data not shown) after BDL. mRNA levels of hepatocyte growth factor (HGF) and heparin-binding ep-

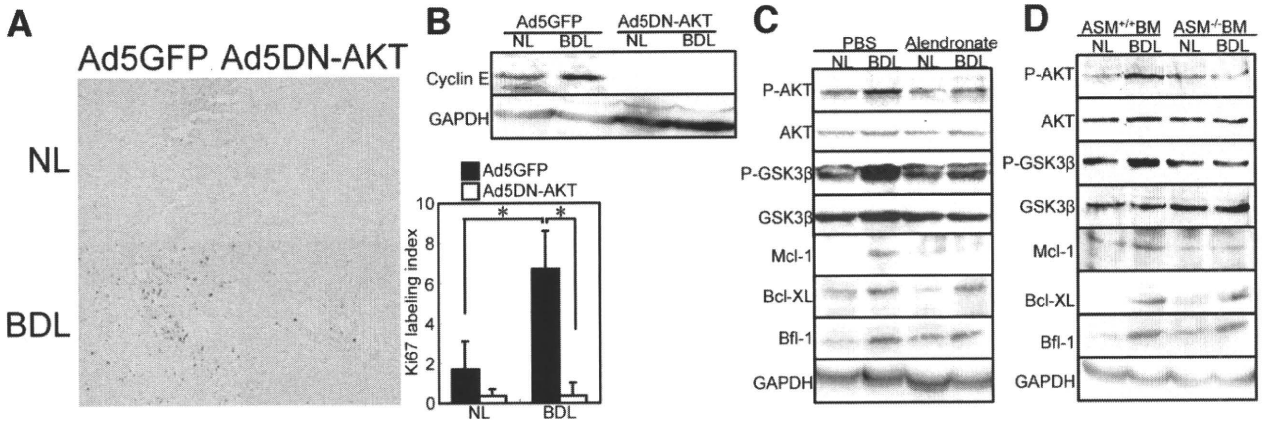

Fig. 7. Kupffer cells and its ASMase are required for AKT activation by BDL. Wildtype mice underwent PBDL and were infected with Ad5GFP or Ad5DN-AKT (A,B) or were treated with Ale-lip or PBS-lip (C). The ASMase$^{+/+}$ bone marrow or ASMase$^{-/-}$ bone marrow-transplanted mice were operated on with PBDL (D). The animals were killed 10 days after the surgery. Expression of Ki67 in the NL right (upper panel) and BDL left (lower panel) lobes were examined by immunohistochemistry (A). (Original magnification ×200.) Ki67 indexes were compared (right panel). Data are means ± SD from at least four independent experiments. *$P < 0.05$ using Student's t test. (B-D) The protein extracts from the livers were subjected to SDS-PAGE and immunoblotting was performed with anti-cyclin E, GAPDH, phosphorylated-AKT, AKT, phosphorylated-GSK3β, GSK3β, Mcl-1, Bcl-XL, and Bfl-1 antibodies. The results shown are representative of at least three independent experiments.

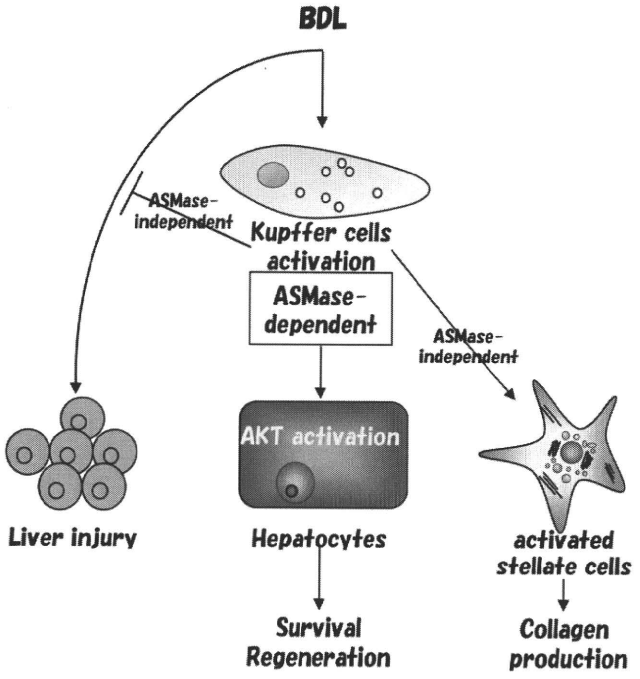

Fig. 8. Hypothetical relations between Kupffer cells and other cells.

ithelial growth factor (HB-EGF), which induce hepatocyte proliferation,[31,32] were not changed in ASMase$^{-/-}$ bone marrow-transplanted mice (Supporting Fig. 7). Accumulation of CD3-positive T cells in BDL lobes in ASMase$^{-/-}$ bone marrow-transplanted mice was also similar to those in ASMase$^{+/+}$ bone marrow-transplanted mice (data not shown). The factors that lead to AKT-dependent hepatocyte protection and regeneration are currently unknown. Further studies are needed to determine these factors.

ASMase has various roles in both parenchymal and nonparenchymal cells. ASMase in hepatocytes modulates hepatocyte apoptosis.[18] Although ASMase in Kupffer cells did not contribute to liver fibrosis, ASMase in HSCs promotes collagen production. Administration of ASMase to human HSCs increased collagen expression. ASMase plus TGF-β treatment further increased collagen production in HSCs (Supporting Fig. 8A). The collagen expression by ASMase is, at least in part, stimulated by way of the modulation of intracellular signals, Smad2/3, downstream targets of TGF-β receptor, and p38, which increases collagen α1(I) mRNA stability in HSCs.[33] The administration of ASMase also phosphorylated p38 (Supporting Fig. 8B). Moreover, exogenous membrane permeable ceramide exerts a stimulatory effect of basal and TGF-β-induced collagen promoter activity in foreskin fibroblast.[34]

In conclusion, Kupffer cells regulate liver injury, hepatocyte survival, regeneration, and fibrosis after chronic liver damage by BDL. AKT activation in hepatocytes, which is induced by way of ASMase of Kupffer cells, is required for the survival and regeneration of hepatocytes. The hypothetical roles of Kupffer cells are schematically summarized in Fig. 8.

References

1. Hirose M, Nishikawa M, Qian W, Haque A, Mashimo M, Inoue M. Mannose-conjugated alendronate selectively depletes Kupffer cells and inhibits endotoxemic shock in the mice. Hepatol Res 2006;36:3-10.
2. Kresse M, Latta M, Kunstle G, Riehle HM, van Rooijen N, Hentze H, et al. Kupffer cell-expressed membrane-bound TNF mediates melphalan hepatotoxicity via activation of both TNF receptors. J Immunol 2005;175:4076-4083.
3. He Q, Kim J, Sharma RP. Fumonisin B1 hepatotoxicity in mice is attenuated by depletion of Kupffer cells by gadolinium chloride. Toxicology 2005;207:137-147.
4. Prins HA, Meijer C, Boelens PG, Diks J, Holtz R, Masson S, et al. Kupffer cell-depleted rats have a diminished acute-phase response following major liver resection. Shock 2004;21:561-565.
5. Ju C, Reilly TP, Bourdi M, Radonovich MF, Brady JN, George JW, et al. Protective role of Kupffer cells in acetaminophen-induced hepatic injury in mice. Chem Res Toxicol 2002;15:1504-1513.
6. Roberts RA, Ganey PE, Ju C, Kamendulis LM, Rusyn I, Klaunig JE. Role of the Kupffer cell in mediating hepatic toxicity and carcinogenesis. Toxicol Sci 2007;96:2-15.
7. Tacke F, Luedde T, Trautwein C. Inflammatory pathways in liver homeostasis and liver injury. Clin Rev Allergy Immunol 2009;36:4-12.
8. Nagata K, Suzuki H, Sakaguchi S. Common pathogenic mechanism in development progression of liver injury caused by non-alcoholic or alcoholic steatohepatitis. J Toxicol Sci 2007;32:453-468.
9. Canbay A, Feldstein AE, Higuchi H, Werneburg N, Grambihler A, Bronk SF, et al. Kupffer cell engulfment of apoptotic bodies stimulates death ligand and cytokine expression. HEPATOLOGY 2003;38:1188-1198.
10. Gehring S, Dickson EM, San Martin ME, van Rooijen N, Papa EF, Harty MW, et al. Kupffer cells abrogate cholestatic liver injury in mice. Gastroenterology 2006;130:810-822.
11. Seki E, De Minicis S, Osterreicher CH, Kluwe J, Osawa Y, Brenner DA, et al. TLR4 enhances TGF-beta signaling and hepatic fibrosis. Nat Med 2007;13:1324-1332.
12. Hannun YA. Functions of ceramide in coordinating cellular responses to stress. Science 1996;274:1855-1859.
13. Bollinger CR, Teichgraber V, Gulbins E. Ceramide-enriched membrane domains. Biochim Biophys Acta 2005;1746:284-294.
14. Sakata A, Ochiai T, Shimeno H, Hikishima S, Yokomatsu T, Shibuya S, et al. Acid sphingomyelinase inhibition suppresses lipopolysaccharide-mediated release of inflammatory cytokines from macrophages and protects against disease pathology in dextran sulphate sodium-induced colitis in mice. Immunology 2007;122:54-64.
15. Dhami R, He X, Gordon RE, Schuchman EH. Analysis of the lung pathology and alveolar macrophage function in the acid sphingomyelinase—deficient mouse model of Niemann-Pick disease. Lab Invest 2001;81:987-999.
16. Utermohlen O, Karow U, Lohler J, Kronke M. Severe impairment in early host defense against Listeria monocytogenes in mice deficient in acid sphingomyelinase. J Immunol 2003;170:2621-2628.
17. Garcia-Ruiz C, Colell A, Mari M, Morales A, Calvo M, Enrich C, et al. Defective TNF-alpha-mediated hepatocellular apoptosis and liver damage in acidic sphingomyelinase knockout mice. J Clin Invest 2003;111:197-208.
18. Osawa Y, Uchinami H, Bielawski J, Schwabe RF, Hannun YA, Brenner DA. Roles for C16-ceramide and sphingosine 1-phosphate in regulating hepatocyte apoptosis in response to tumor necrosis factor-alpha. J Biol Chem 2005;280:27879-27887.

19. Osawa Y, Seki E, Adachi M, Taura K, Kodama Y, Siegmund SV, et al. Systemic mediators induce fibrogenic effects in normal liver after partial bile duct ligation. Liver Int 2006;26:1138-1147.
20. Osawa Y, Hannun YA, Proia RL, Brenner DA. Roles of AKT and sphingosine kinase in the antiapoptotic effects of bile duct ligation in mouse liver. HEPATOLOGY 2005;42:1320-1328.
21. Osawa Y, Nagaki M, Banno Y, Brenner DA, Nozawa Y, Moriwaki H, et al. Expression of the NF-kappa B target gene X-ray-inducible immediate early response factor-1 short enhances TNF-alpha-induced hepatocyte apoptosis by inhibiting Akt activation. J Immunol 2003;170:4053-4060.
22. Sokol RJ, Devereaux M, Dahl R, Gumpricht E. "Let there be bile"—understanding hepatic injury in cholestasis. J Pediatr Gastroenterol Nutr 2006;43(Suppl 1):S4-S9.
23. Yerushalmi B, Dahl R, Devereaux MW, Gumpricht E, Sokol RJ. Bile acid-induced rat hepatocyte apoptosis is inhibited by antioxidants and blockers of the mitochondrial permeability transition. HEPATOLOGY 2001;33:616-626.
24. Higuchi H, Gores GJ. Bile acid regulation of hepatic physiology: IV. Bile acids and death receptors. Am J Physiol Gastrointest Liver Physiol 2003; 284:G734–738.
25. Jaeschke H. Inflammation in response to hepatocellular apoptosis. HEPATOLOGY 2002;35:964-966.
26. Canbay A, Higuchi H, Bronk SF, Taniai M, Sebo TJ, Gores GJ. Fas enhances fibrogenesis in the bile duct ligated mouse: a link between apoptosis and fibrosis. Gastroenterology 2002;123:1323-1330.
27. Minter RM, Fan MH, Sun J, Niederbichler A, Ipaktchi K, Arbabi S, et al. Altered Kupffer cell function in biliary obstruction. Surgery 2005;138: 236-245.
28. Gressner AM. Cytokines and cellular crosstalk involved in the activation of fat-storing cells. J Hepatol 1995;22:28-36.
29. Bataller R, Brenner DA. Liver fibrosis. J Clin Invest 2005;115:209-218.
30. Mullany LK, Nelsen CJ, Hanse EA, Goggin MM, Anttila CK, Peterson M, et al. Akt-mediated liver growth promotes induction of cyclin E through a novel translational mechanism and a p21-mediated cell cycle arrest. J Biol Chem 2007;282:21244-21252.
31. Ueki T, Kaneda Y, Tsutsui H, Nakanishi K, Sawa Y, Morishita R, et al. Hepatocyte growth factor gene therapy of liver cirrhosis in rats. Nat Med 1999;5:226-230.
32. Kiso S, Kawata S, Tamura S, Inui Y, Yoshida Y, Sawai Y, et al. Liver regeneration in heparin-binding EGF-like growth factor transgenic mice after partial hepatectomy. Gastroenterology 2003;124:701-707.
33. Tsukada S, Westwick JK, Ikejima K, Sato N, Rippe RA. SMAD and p38 MAPK signaling pathways independently regulate alpha collagen(I) gene expression in unstimulated and transforming growth factor-beta-stimulated hepatic stellate cells. J Biol Chem 2005;280:10055-10064.
34. Sato M, Markiewicz M, Yamanaka M, Bielawska A, Mao C, Obeid LM, et al. Modulation of transforming growth factor-beta (TGF-beta) signaling by endogenous sphingolipid mediators. J Biol Chem 2003;278:9276-9282.

ELSEVIER

Nutrition 26 (2010) 269–275

NUTRITION

www.nutritionjrnl.com

Applied nutritional investigation

Elevated serum tumor necrosis factor-α and soluble tumor necrosis factor receptors correlate with aberrant energy metabolism in liver cirrhosis

Makoto Shiraki, M.D., Ph.D.[a,*], Yoichi Terakura, M.D.[a], Junpei Iwasa, M.D.[a], Masahito Shimizu, M.D., Ph.D.[a], Yoshiyuki Miwa, M.D., Ph.D.[a], Nobuo Murakami, M.D., Ph.D.[b], Masahito Nagaki, M.D., Ph.D.[a], and Hisataka Moriwaki, M.D., Ph.D.[a]

[a]*Department of Internal Medicine, Gifu University School of Medicine, Yanagido, Gifu, Japan*
[b]*Center for Nutrition Support & Infection Control, Gifu University Hospital, Yanagido, Gifu, Japan*

Manuscript received November 4, 2008; accepted April 22, 2009.

Abstract

Objective: Protein–energy malnutrition is frequently observed in patients with liver cirrhosis and is associated with their poor prognosis. Tumor necrosis factor-α (TNF-α) is elevated in those patients and may contribute to the alterations of energy metabolism. Our aim was to characterize the aberrant energy metabolism in cirrhotic patients with regard to TNF-α.

Methods: Twenty-four patients (mean age 65 ± 6 y) with viral liver cirrhosis who did not have hepatocellular carcinoma or acute infections were studied. Twelve healthy volunteers were recruited after matching for age, gender, and body mass index with the patients and served as controls (59 ± 8 y). Serum levels of TNF-α, soluble 55-kDa TNF receptor (sTNF-R55), soluble 75-kDa TNF receptor (sTNF-R75), and leptin were determined by immunoassay. Substrate oxidation rates of carbohydrate and fat were estimated by indirect calorimetry after overnight bedrest and fasting.

Results: In cirrhotic patients, serum levels of TNF-α, sTNF-R55, and sTNF-R75 were significantly higher than those in the controls and correlated with the increasing grade of disease severity as defined by Child-Pugh classification. Serum leptin concentration was not different between cirrhotics and controls but correlated with their body mass index. The decrease in substrate oxidation rate of carbohydrate and the increase in substrate oxidation rate of fat significantly correlated with serum TNF-α, sTNF-R55, and sTNF-R75 concentrations.

Conclusion: Tumor necrosis factor-α might be associated with the aberrant energy metabolism in patients with liver cirrhosis.

Keywords: Liver cirrhosis; Tumor necrosis factor-α; Soluble 55-kDa tumor necrosis factor receptor; soluble 75-kDa tumor necrosis factor receptor; Leptin; Indirect calorimetry; Protein–energy malnutrition

Introduction

A significant proportion of patients with liver cirrhosis shows protein–energy malnutrition (PEM) [1,2], and PEM leads to poor prognosis in these cases [3–5]. Energy metabolism and nutritional status can be estimated, for example, by indirect calorimetry [5,6] and by anthropometry, such as triceps skinfold thickness (TSF) and arm muscle circumference (AMC) [7]. Impaired energy metabolism significantly correlates with a worse event-free survival of cirrhotics [5,7,8]. However, the mechanisms underlying energy malnutrition in cirrhosis have not been elucidated enough [2]. Candidate causes for this state include enhanced secretion of cytokines such as tumor necrosis factor-α (TNF-α) and adipokines represented by leptin in liver cirrhosis, because both induce anorexia and increase energy expenditure, leading to physical wasting [9–11].

Tumor necrosis factor-α, or cachectin, is a proinflammatory cytokine and is released mainly from monocytes and lymphocytes in response to inflammatory stimuli [12]. TNF-α is also postulated to play a role in the development of anorexia or physical wasting and to regulate energy

*Corresponding author. Tel.: +81-58-230-6308; fax: +81-58-230-6310.
E-mail address: mshiraki-gif@umin.ac.jp (M. Shiraki).

0899-9007/10/$ – see front matter
doi:10.1016/j.nut.2009.04.016

Table 1
Baseline demographic characteristics, body composition, blood biochemistry, and calorimetric data in cirrhotic patients and control subjects*

	Controls ($n = 12$)	Cirrhosis ($n = 24$)	$P^{\dagger}$	Child A ($n = 9$)	Child B ($n = 9$)	Child C ($n = 6$)	$P^{\ddagger}$
Age (y)	58.5 (48–68)	64 (64–75)	0.31	63 (58–69)	67 (63–75)	61 (54–76)	0.10
Male/female	8/4	16/8	0.58	6/3	5/4	5/1	0.90
Height (cm)	168 (153–175)	159 (143–173)	<0.05	159 (145–170)	156 (143–166)	161 (144–173)	0.67
Weight (kg)	62 (54–66)	59 (47–87)	0.36	64 (48–74)	56 (39–67)	59 (47–87)	0.51
Body mass index (kg/m^2)	22.0 (20.8–24.3)	21.3 (17.3–26.9)	0.42	22.9 (19.0–26.9)	22.1 (17.0–29.0)	18.5 (17.7–22.5)	0.11
Arm muscle circumference (%)	101 (85–107)	96 (78–107)	0.59	104 (87–112)	91 (72–108)	95 (78–105)	<0.01
Triceps skinfold thickness (%)	139 (82–200)	92 (46–180)	<0.01	104 (84–181)	92 (46–138)	80 (55–168)	0.05
Total bilirubin (mg/dL)	0.7 (0.4–0.9)	1.4 (0.7–6.6)	<0.01	1.2 (0.7–1.9)	1.4 (0.4–2.5)	3.5 (1.4–6.5)	<0.01
Albumin (g/dL)	4.6 (4.2–4.8)	3.1 (2.4–4.4)	<0.01	3.3 (2.4–4.4)	3.0 (2.5–3.3)	2.8 (2.0–3.4)	0.07
Alanine aminotransferase (IU/L)	18 (8–25)	50 (22–140)	<0.01	71 (22–140)	39 (26–106)	46 (38–69)	0.10
Prothrombin time (%)	98 (94–102)	69 (30–150)	<0.01	83 (55–150)	62 (47–87)	50 (30–65)	<0.01
TNF-α (ng/L)	3.0 (2.0–3.5)	8.3 (5.0–19.0)	<0.01	6.6 (5.0–11.0)	9.4 (7.4–15.1)	12.3 (7.0–19.0)	<0.01
sTNF-R55 (ng/L)	1025 (773–1450)	2505 (1390–5000)	<0.01	1575 (1350–5000)	2680 (2000–5000)	3240 (2840–5000)	<0.01
sTNF-R75 (ng/L)	1805 (1460–2360)	4255 (1840–5000)	<0.01	3210 (1840–5000)	4900 (3920–5000)	4800 (4000–5000)	<0.01
Leptin (μg/L)	4.3 (3.2–5.4)	4.7 (1.5–17.5)	0.95	6.3 (2.9–17.5)	3.8 (1.5–13.9)	2.8 (1.7–8.3)	0.09
REE (kcal/d)	1330 (1140–1450)	1188 (892–1830)	0.41	1507 (981–1830)	1188 (1011–1826)	1655 (1011–1342)	0.36
BMR (kcal/d)	1355 (1163–1428)	1170 (1077–1760)	0.09	1250 (1110–1530)	1160 (850–1380)	1170 (1077–1760)	0.47
npRQ	0.91 (0.87–0.94)	0.84 (0.70–0.97)	<0.01	0.88 (0.84–0.97)	0.83 (0.77–0.86)	0.75 (0.70–0.80)	<0.01
CHO (%)	50.4 (42.0–56.3)	39.9 (18.4–61.6)	<0.01	42.3 (25.7–61.6)	39.7 (18.4–48.7)	25.4 (19.9–30.6)	<0.01
FAT (%)	29.1 (22.6–37.2)	37.5 (23.0–61.6)	<0.01	31.0 (25.9–53.9)	38.0 (23.0–55.5)	61.0 (45.9–61.6)	<0.01
PRO (%)	20.7 (11.6–26.4)	22.7 (5.2–32.3)	0.43	23.8 (11.8–33.0)	25.2 (5.2–32.3)	14.5 (12.9–23.5)	0.08

BMR, basal metabolic rate predicted by the Harris-Benedict formula; Child, Child-Pugh grade; CHO, substrate oxidation rate of carbohydrate; FAT, substrate oxidation rate of fat; PRO, substrate oxidation rate of protein; REE, resting energy expenditure; TNF-α, tumor necrosis factor-α; npRQ, non-protein respiratory quotient; sTNF-R55, soluble 55-kDa tumor necrosis factor receptor; sTNF-R75, soluble 75-kDa tumor necrosis factor receptor.

* Values are expressed as median (range).

† Between controls and cirrhosis by Fisher's exact test or Mann-Whitney U test.

‡ For distribution among Child-Pugh grades by chi-square test or one-way analysis of variance.

metabolism [9,10]. The actions of TNF-α are mediated by two distinct cell-surface receptors, soluble 55-kDa tumor necrosis factor receptor (sTNF-R55) and soluble 55-kDa tumor necrosis factor receptor (sTNF-R75) [12–14]. These two receptors also exist in soluble form after their extracellular domains have been cleaved proteolytically from the cell surface. These soluble receptors can block TNF-α activity by competing with cell-surface TNFR or prolong the biological effect of TNF-α as a buffer system. Because circulating TNFR levels remain elevated for a longer period than TNF-α, it is proposed that sTNFR levels may serve as a more sensitive means of monitoring the activity of the TNF-α system. In previous reports, serum TNF-α, sTNF-R55, and sTNF-R75 concentrations were elevated in cirrhotic patients [15,16], correlating with severity of liver damage [16–18]. However, little has been studied regarding the relation between TNF-α and alternations of energy metabolism in cirrhosis [19].

Leptin, a 16-kDa protein product by adipocytes, is postulated to regulate energy balance by suppressing appetite and increasing energy expenditure [11]. In several studies, serum leptin concentrations were elevated in cirrhotic patients, which suggested that leptin might play a role in the development of anorexia or physical wasting associated with cirrhosis [20–22].

Thus, in this study we aimed to test whether elevated serum concentrations of TNF-α, sTNF-R55, sTNF-R75, and leptin are associated with the aberrant energy metabolism in patients with liver cirrhosis.

Materials and methods

Patients

Twenty-four patients with liver cirrhosis (16 men and 8 women, mean age 65 ± 6 y) participated in this study. Liver cirrhosis was diagnosed by clinical and laboratory profiles and by histologic examination of liver biopsy specimens. Child-Pugh grade of disease severity [23] was A in nine cases, B in nine cases, and C in six cases. Hepatitis C virus was the cause of cirrhosis in all cases. Patients with physically detectable ascites or peripheral edema of moderate to severe grade [8] were excluded. Patients with hepatocellular carcinoma, fever, human immunodeficiency virus infection, overt infectious disease (septicemia, pneumonia, urinary tract infection), renal insufficiency, or under immunomodulatory therapy were also excluded. Clinical profiles of the patients are presented in Table 1. Twelve healthy volunteers were recruited after matching for age, gender, and body mass index (BMI) with the patients and served as controls (eight men and four women, mean age 59 ± 8 y). The study protocol was approved by the institutional review board for human research, and informed consent was obtained from all participants. The study protocol was in agreement with the 1975 Helsinki Declaration as revised in 1983. We matched the patients and the controls not only by age and gender but also by BMI, because obesity is reported to affect significantly the histologic grade of hepatic fat deposition, inflammation, and fibrosis even in

chronic viral hepatitis [24,25], thus reducing the functional reserve of the liver.

Methods

Blood was drawn in the early morning for fasting serum concentrations of TNF-α, sTNF-R55, sTNF-R75, leptin, and routine laboratory examinations on the day of metabolic studies. Serum albumin, total bilirubin, alanine aminotransferase, prothrombin activity, and urinary nitrogen (UN) were measured with a standard clinical analyzer at the central laboratory in our hospital. Serum TNF-α, sTNF-R55, and sTNF-R75 were determined in duplicate with an enzyme-linked immunosorbent assay (R&D Systems, Minneapolis, MN, USA). Serum leptin was measured in duplicate by radioimmunoassay (Linco Research, Inc., St. Louis, MO, USA).

Metabolic studies were carried out using an indirect calorimeter (Deltatrac Metabolic Monitor, Datax Division Instrumentarium Corp., Helsinki, Finland) to estimate non-protein respiratory quotient (npRQ), resting energy expenditure (REE), and substrate oxidation rates of carbohydrate (%CHO), fat (%FAT), and protein (%PRO) from measured oxygen consumption per minute (Vo_2), carbon dioxide production per minute (Vco_2) and total UN using the following equations [26–28].

$$REE = 5.50\ Vo_2 + 1.76\ Vco_2 - 1.99\ UN$$

$$CHO(g/24\ h) = 5.926\ Vo_2 - 4.189\ Vco_2 - 2.539\ UN$$

$$FAT(g/24\ h) = 2.432\ Vo_2 - 2.432\ Vco_2 - 1.943\ UN$$

$$PRO(g/24\ h) = 6.250\ UN$$

$$npRQ = (1.44 \times Vco_2 - 4.890\ UN)/(1.44 \times Vo_2 - 6.04\ UN)$$

$$\%CHO = CHO \times 4.18/REE \times 100$$

$$\%FAT = FAT \times 9.46/REE \times 100$$

$$\%PRO = PRO \times 4.32/REE \times 100$$

Measurements were performed between 07:00 and 09:00 h while the patients were still lying in bed. The last meal was served 18:00 h on the previous day. The basal metabolic rate was predicted by the Harris-Benedict formula [29].

We measured height and body weight and calculated BMI. Arm circumference and TSF were measured with an Insertape and Adipometer (Abbott Japan Co., Ltd., Tokyo, Japan), and AMC was estimated. Anthropometric data were standardized according to age- and gender-stratified Japanese anthropometric reference data [30] and expressed as percentages of TSF and AMC.

Statistical analysis

Values were expressed as median and range. Comparisons between groups were analyzed using Mann-Whitney U or Kruskal-Wallis non-parametric test. Comparison between measured REE and corresponding Harris-Benedict prediction was performed by paired *t* test. The relation among blood test parameters and substrate oxidation rates or Child-Pugh grade was determined by Spearman's correlation.

All analyses were carried out using JMP 5.0 (SAS Institute, Cary, NC, USA) and statistical significance was accepted at $P < 0.05$.

Results

Serum concentrations of TNF-α, sTNF-R55, sTNF-R75, and leptin

Cirrhotic patients had significantly lower %TSF and %AMC in parallel with the increasing Child-Pugh score (Table 1), suggesting the presence of PEM in these subjects.

The median serum concentrations of TNF-α, sTNF-R55, and sTNF-R75 were significantly higher in cirrhotic patients than in controls (Table 1). Serum TNF-α, sTNF-R55, and sTNF-R75 levels correlated with the increasing grade of disease severity as defined by the Child-Pugh classification in patients with liver cirrhosis (Table 1, Fig. 1).

Serum leptin concentration did not differ between cirrhotic patients and controls or correlate with Child-Pugh score (Table 1), but correlated with their BMI (Fig. 2).

Energy metabolism

Measured REE (1188 kcal/d, 892–1830 kcal/d) was significantly higher than the basal metabolic rate (1170 kcal/d, 1077–1760 kcal/d) predicted by the Harris-Benedict formula in liver cirrhosis ($P < 0.01$), whereas both agreed well in control subjects.

The npRQ in patients with liver cirrhosis (0.84, 0.70–0.97) was significantly lower than that in control subjects (0.91, 0.87–0.94, $P < 0.01$). Decrease in npRQ was brought about by a significantly lower oxidation rate of carbohydrate and a higher oxidation rate of fat in patients with liver cirrhosis compared with control subjects (Fig. 3). A decrease in %CHO and an increase in %FAT significantly correlated with the progression of disease severity in patients with liver cirrhosis as defined by the Child-Pugh classification (Fig. 3).

Correlation between serum cytokine levels and oxidation rates of nutrients in patients with liver cirrhosis

Inverse correlations were found between %CHO and serum concentrations of TNF-α, sTNF-R55, and sTNF-R75 (Fig. 4, Table 2). Significant correlations were observed between %FAT and serum concentrations of TNF-α, sTNF-R55,

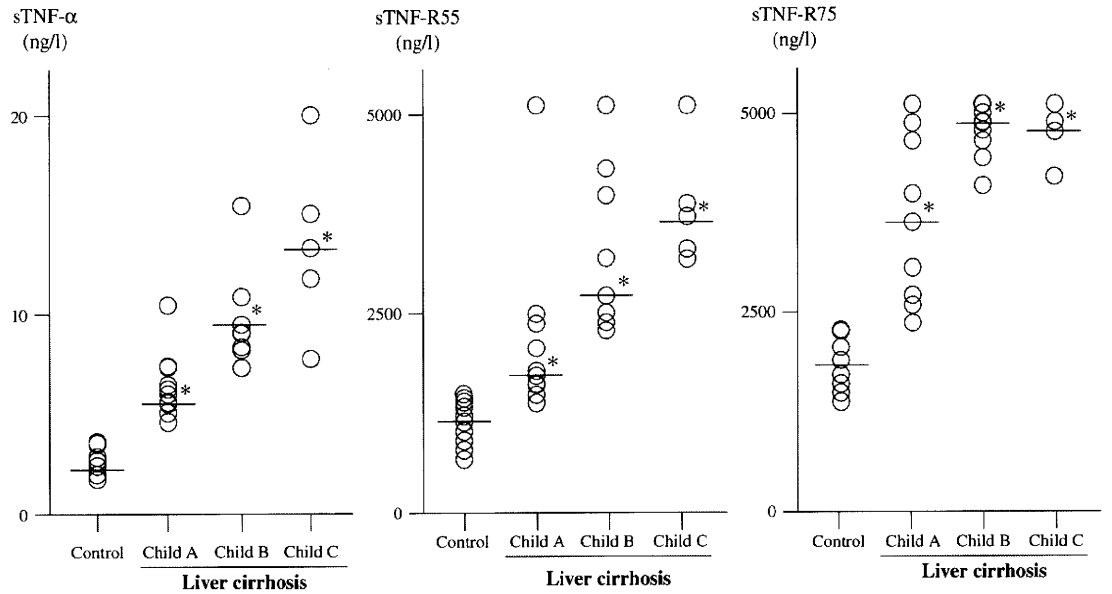

Fig. 1. Serum levels of TNF-α, sTNF-R55, and sTNF-R75 in control subjects ($n = 12$) and in patients with liver cirrhosis ($n = 24$) graded by Child-Pugh classification ($n = 9, 9$, and 6 for grades A, B, and C, respectively). Horizontal line indicates the median. * $P < 0.05$ compared with control. Child, Child-Pugh grade; sTNF-R55, soluble 55-kDa tumor necrosis factor receptor; sTNF-R75, soluble 75-kDa tumor necrosis factor receptor receptor; TNF-α, tumor necrosis factor-α.

and sTNF-R75 (Fig. 5, Table 2). However, %PRO did not correlate with serum concentrations of these cytokines.

Other intercorrelations among cytokines, leptin, substrate oxidation rates, and Child- Pugh grade in patients with liver cirrhosis are presented in Table 2. Serum leptin did not correlate with %CHO or %FAT. Serum leptin did not correlate with TNF-α, sTNF-R55, or sTNF-R75.

Correlations of serum cytokine and leptin levels with parameters of liver damage in cirrhotic patients

The serum concentrations of TNF-α, sTNF-R55, and sTNF-R75 correlated significantly with Child-Pugh score

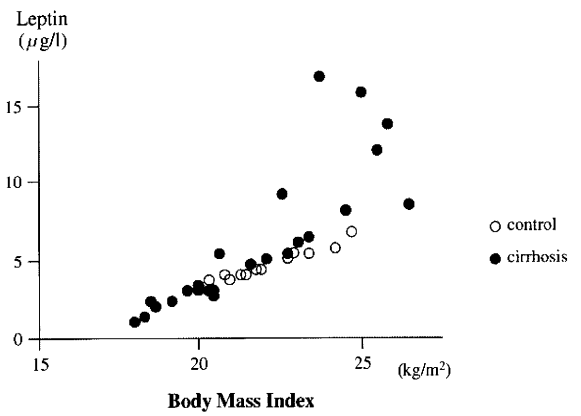

Fig. 2. Correlation between body mass index and serum leptin level in cirrhotic patients (closed circles) and controls (open circles; $n = 36$, $r = 0.735$, $P < 0.05$).

(Table 2), prothrombin time, total bilirubin, and albumin in patients with liver cirrhosis. However, serum leptin level showed no correlation with such parameters (data not shown).

Discussion

Because the liver plays a central role in fuel and energy metabolism, PEM is common in patients with liver cirrhosis [1,2]. Recently, several studies have elucidated the relation between PEM and event-free survival in patients with liver cirrhosis [3–5,31,32]. Thus, PEM is an important outcome marker and a therapeutic target in cirrhotic patients.

It has been reported that the fasting oxidation rate of glucose is decreased and that of fat is increased in patients with liver cirrhosis [5,6,26]. Such aberrant energy metabolism consequently decreases npRQ in cirrhotics [5,6,26]. It also has been reported that this decrease of npRQ closely correlates with survival in patients with liver cirrhosis [5]. As confirmed in this study, npRQ in liver cirrhosis was significantly lower than that in control subjects. The decrease in npRQ was brought about by a significantly lower oxidation rate of carbohydrate and higher oxidation rate of fat in patients with liver cirrhosis compared with control subjects. A decrease in %CHO and an increase in %FAT significantly correlated with the progression of disease severity in patients with liver cirrhosis as defined by the Child-Pugh classification. These characteristics of energy metabolism in liver cirrhosis agree well with those in previous reports [5,6,26], suggesting that the patients recruited in the present study can be regarded as representative of a general cirrhotic cohort. Regarding

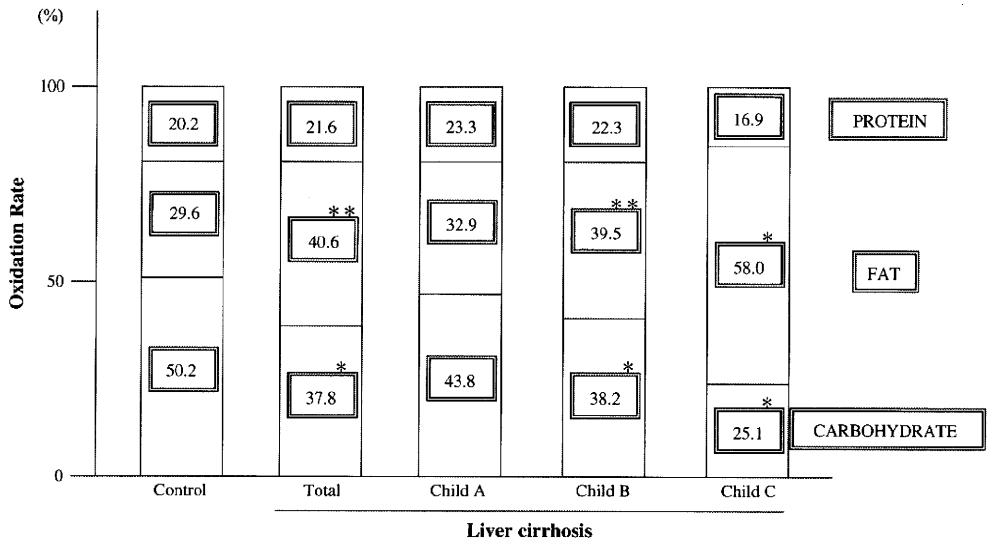

Fig. 3. Substrate oxidation rates of protein, fat, and carbohydrate in control subjects ($n = 12$) and in patients with liver cirrhosis ($n = 24$) graded by Child-Pugh classification ($n = 9$, 9, and 6 for grades A, B, and C, respectively). Values are expressed as mean. * $P < 0.05$, ** $P < 0.01$ compared with control. Child, Child-Pugh grade.

%TSF as another parameter of energy nutrition, the patients actually showed a significantly lower value than the controls with a similar BMI. However, we should point out the possibility that the patients could have had an overestimated BMI due to the presence of excess fluid before the appearance of detectable ascites or moderate to severe peripheral edema.

Tumor necrosis factor-α is a proinflammatory cytokine and postulated to regulate energy metabolism [9,10,33]. In previous reports, TNF-α increased glucose (~10%) and free fatty acid (~126%) turnover and raised REE (~34%) [9,10,33]. The actions of TNF-α are mediated by two distinct cell-surface receptors. We measured not only serum TNF-α concentration but also sTNF-R55 and sTNF-R75 concentrations for a couple of reasons. First, it is known that sTNF-R shedding is induced by the same stimuli that activate TNF-α production. Second, it has been shown that sTNF-R levels remain elevated for a longer time than TNF-α itself. Taken together, sTNF-R levels could confirm the stimulated state of the TNF-α system and could reflect the state until later after stimuli.

In this study, serum TNF-α, sTNF-R55, and sTNF-R75 concentrations were significantly higher in cirrhotic patients

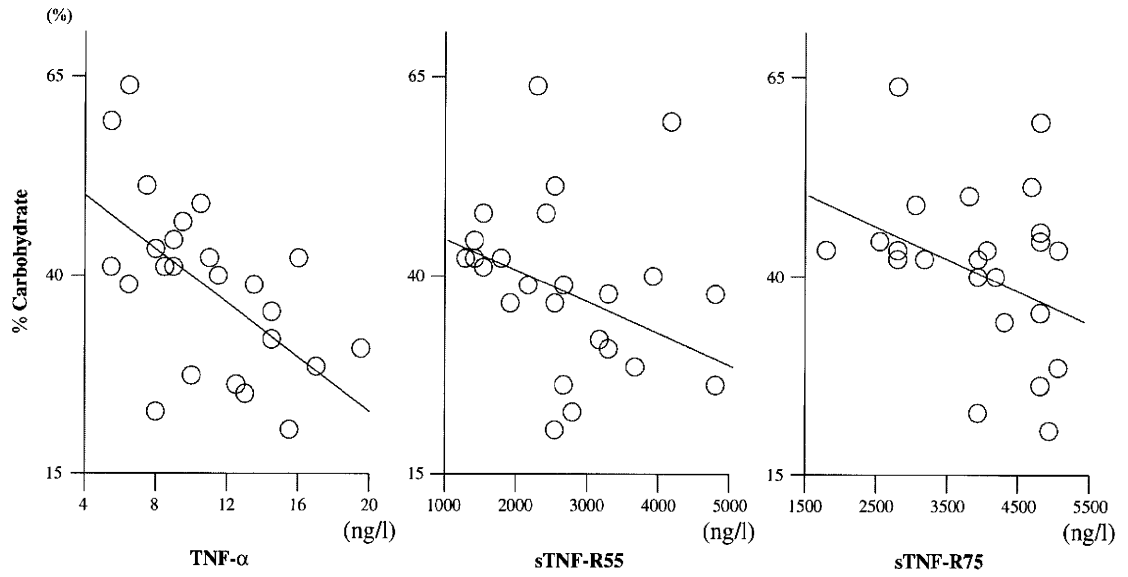

Fig. 4. Correlation between the oxidation rate of carbohydrate and serum TNF-α, sTNF-R55, or sTNF-R75 in patients with liver cirrhosis ($n = 24$). For correlation coefficients and statistical significance, see Table 2. sTNF-R55, soluble 55-kDa tumor necrosis factor receptor; sTNF-R75, soluble 75-kDa tumor necrosis factor receptor receptor; TNF-α, tumor necrosis factor-α.

Table 2
Intercorrelation coefficients among cytokines, leptin, substrate oxidation rates, and Child-Pugh score in patients with liver cirrhosis

	TNF-α	sTNF-R55	sTNF-R75	%CHO	%FAT	Leptin
sTNF-R55	0.32					
sTNF-R75	0.43*	0.85†				
%CHO	−0.56†	−0.44*	−0.41*			
%FAT	0.72†	0.61†	0.61†	−0.82†		
Leptin	−0.15	−0.01	0.06	0.08	−0.02	
Child-Pugh score	0.63†	0.61†	0.61†	−0.64†	0.78†	−0.36

%CHO, substrate oxidation rate of carbohydrate; %FAT, substrate oxidation rate of fat; TNF-α, tumor necrosis factor-α; sTNF-R55, soluble 55-kDa tumor necrosis factor receptor; sTNF-R75, soluble 75-kDa tumor necrosis factor receptor.

* $P < 0.05$.

† $P < 0.01$.

than in controls, and they correlated with the increasing grade of disease severity as defined by the Child-Pugh classification in patients with liver cirrhosis. Among damaged liver functions in cirrhosis, the high activity of the TNF-α system may particularly be related to a decrease in hepatic clearance of endotoxins, the presence of portosystemic shunts, and the systemic spillover of intestinal endotoxins by portal hypertension [15,34]. Another explanation is that the presence of chronic viral inflammation could be the reason for the elevated proinflammatory cytokines including TNF-α [35,36].

Moreover, inverse correlations were found between %CHO and serum concentrations of TNF-α, sTNF-R55, and sTNF-R75 in this study. Significant correlations were observed between %FAT and serum concentrations of TNF-α, sTNF-R55, and sTNF-R75. As described previously, TNF-α induces free fatty acid oxidation more efficiently than glucose oxidation [6,9,10]. In addition, the production of adenosine triphosphate by β-oxidation of free fatty acids is much greater than that by glucose oxidation. Hence, TNF-α seems to raise %FAT more directly and to contribute to whole aberrant energy metabolism subsequently in liver cirrhosis by altering the proportion of fat oxidation to carbohydrate oxidation.

Serum leptin is another candidate factor to alter energy balance by its wasting action and is reported to be actually high in patients with liver cirrhosis [11,20–22]. However, in this study, serum leptin concentration did not differ between cirrhotic patients and controls. Moreover, serum leptin level showed no correlation with energy metabolism parameters measured by indirect calorimetry. Most previous studies regarding leptin recruited patients with alcoholic cirrhosis [20,22], whereas all patients in our investigation had cirrhosis caused by hepatitis C virus. This difference in the cause of liver damage may account for the disagreement between previous reports and the present one.

Regarding the correlation between TNF and aberrant energy metabolism, we should point out a possibility that the correlation may merely arise from an association between cytokine levels and Child-Pugh grade, as shown in Figure 1, and that between substrate oxidation rates and the grade, as presented in Table 2. To support our hypothesis that the correlation between TNF and energy metabolism is independent of the degree of liver damage, we statistically tested the relation by confining subjects to those with each Child-Pugh grade. In each subgroup that was controlled for grade, TNF and %FAT retained the significant correlation (e.g., $r = 0.81$, $P < 0.01$ in Child-Pugh grade A). These results strengthen our statement

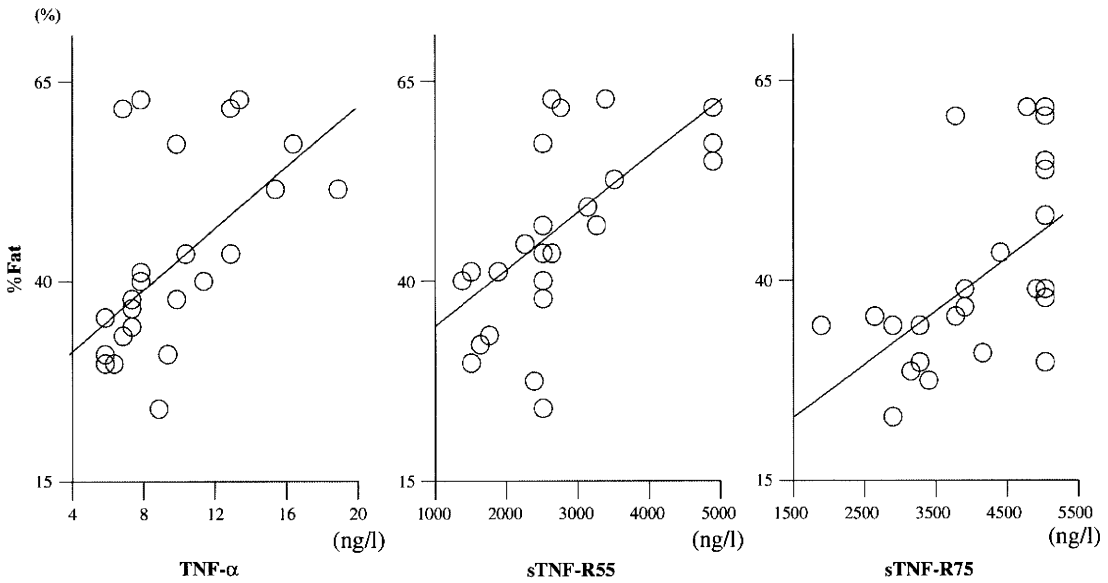

Fig. 5. Correlation between the oxidation rate of fat and serum TNF-α, sTNF-R55, or sTNF-R75 in patients with liver cirrhosis ($n = 24$). For correlation coefficients and statistical significance, see Table 2. sTNF-R55, soluble 55-kDa tumor necrosis factor receptor; sTNF-R75, soluble 75-kDa tumor necrosis factor receptor receptor; TNF-α, tumor necrosis factor-α.

that TNF-α might be associated with aberrant energy metabolism in patients with liver cirrhosis.

Taken together, it seems more likely that the high activity of the TNF-α system mediates the aberrant energy metabolism in patients with liver cirrhosis. To directly demonstrate this possibility, future clinical trials would be required to test whether or not the therapy to decrease the high TNF-α activity might correct the aberrant energy metabolism in patients with liver cirrhosis, by using such modalities as antibiotics and lactulose that control the intestinal bacterial flora or anti–TNF-α antibody.

In summary, the TNF-α system in patients with liver cirrhosis was activated and correlated with disease activity. The significant correlation of serum TNF-α, sTNF-R55, and sTNF-R75 with the aberrant energy metabolism suggested that activation of the TNF-α system contributed to cirrhosis-associated PEM.

References

[1] Morgan AG, McAdam WA, Walmsley GR, Horrocks JC, De Dombal FT. Nutrition in cryptogenic cirrhosis and chronic aggressive hepatitis. Gut 1976;17:113–8.

[2] Müller MJ. Malnutrition in cirrhosis. J Hepatol 1995;23(suppl 1):31–5.

[3] Mendenhall CL, Tosch T, Weesner RE, Garcia-Pont P, Goldberg SJ, Kiernan T, et al. VA cooperative study on alcoholic hepatitis. II: prognostic significance of protein–calorie malnutrition. Am J Clin Nutr 1986;43:213–8.

[4] McCullough AJ, Raguso C. Effect of cirrhosis on energy expenditure. Am J Clin Nutr 1999;69:1066–8.

[5] Tajika M, Kato M, Mohri H, Miwa Y, Kato T, Ohnishi H, et al. Prognostic value of energy metabolism in patients with viral liver cirrhosis. Nutrition 2002;18:229–34.

[6] Miwa Y, Shiraki M, Kato M, Tajika M, Mohri H, Murakami N, et al. Improvement of fuel metabolism by nocturnal energy supplementation in patients with liver cirrhosis. Hepatol Res 2000;18:184–9.

[7] Alberino F, Gatta A, Amodio P, Merkel C, Di Pascoli L, Boffo G, et al. Nutrition and survival in patients with liver cirrhosis. Nutrition 2001; 17:445–50.

[8] Muto Y, Sato S, Watanabe A, Moriwaki H, Suzuki K, Kato A, et al. Effects of oral branched-chain amino acid granules on event-free survival in patients with liver cirrhosis. Clin Gastroenterol Hepatol 2005;3:705–13.

[9] Jin MB, Shimahara Y, Yamaguchi T, Ichimiya M, Kinoshita K, Oka T, et al. The effect of a bolus injection of TNF-alpha and IL-1 beta on hepatic energy metabolism in rats. J Surg Res 1995;58:509–15.

[10] Van der Poll T, Romijn JA, Endert E, Borm JJ, Büller HR, Sauerwein HP. Tumor necrosis factor mimics the metabolic response to acute infection in healthy humans. Am J Physiol 1991;261:457–65.

[11] Zhang Y, Proenca R, Maffei M, Barone M, Leopold L, Friedman JM. Positional cloning of the mouse obese gene and its human homologue. Nature 1994;372:425–32.

[12] Beutler B, Cerami A. Cachectin (tumor necrosis factor): a macrophage hormone governing cellular metabolism and inflammatory response. Endocr Rev 1988;9:57–66.

[13] Tracey KJ, Cerami A. Cerami. Tumor necrosis factor: a pleiotropic cytokine and therapeutic target. Annu Rev Med 1994;45:491–503.

[14] Moldawer LL, Copeland EM III. Proinflammatory cytokines, nutritional support, and the cachexia syndrome: interactions and therapeutic options. Cancer 1997;79:1828–39.

[15] Lee FY, Lu RH, Tsai YT, Lin HC, Hou MC, Li CP, et al. Plasma interleukin-6 levels in patients with cirrhosis. Relationship to endotoxemia, tumor necrosis factor-alpha, and hyperdynamic circulation. Scand J Gastroenterol 1996;31:500–5.

[16] Naveau S, Emilie D, Balian A, Grangeot-Keros L, Borotto E, Portier A, et al. Plasma levels of soluble tumor necrosis factor receptors p55 and p75 in patients with alcoholic liver disease of increasing severity. J Hepatol 1998;28:778–84.

[17] Zylberberg H, Rimaniol AC, Pol S, Masson A, De Groote D, Berthelot P, et al. Soluble tumor necrosis factor receptors in chronic hepatitis C: a correlation with histological fibrosis and activity. J Hepatol 1999;30:185–91.

[18] Moulias R, Meaume S, Raynaud-Simon A. Sarcopenia, hypermetabolism, and aging. Z Gerontol Geriatr 1999;32:425–32.

[19] Marinos G, Naoumov NV, Rossol S, Torre F, Wong PY, Gallati H, et al. Tumor necrosis factor receptors in patients with chronic hepatitis B virus infection. Gastroenterology 1995;108:1453–63.

[20] McCullough AJ, Bugianesi E, Marchesini G, Kalhan SC. Gender-development alternations in serum leptin in alcoholic cirrhosis. Gastroenterology 1998;115:947–53.

[21] Testa R, Franceschini R, Giannini E, Cataldi A, Botta F, Fasoli A, et al. Serum leptin levels in patients with viral chronic hepatitis and liver cirrhosis. J Hepatol 2000;33:33–7.

[22] Nicolás JM, Fernández-Solà J, Fatjó F, Casamitjana R, Bataller R, Sacanella E, et al. Increased circulating leptin levels in chronic alcoholism. Alcohol Clin Exp Res 2001;25:83–8.

[23] Pugh RN, Murray-Lyon IM, Dawson JL, Pietroni MC, Williams R. Transection of the oesophagus for bleeding oesophageal varices. Br J Surg 1973;60:646–9.

[24] Moriwaki H, Shiraki M, Fukushima H, Shimizu M, Iwasa J, Naiki T, et al. Long-term outcome of branched-chain amino acid treatment in patients with liver cirrhosis. Hepatol Res 2008; 38(suppl):S102–6.

[25] Hickman IJ, Clouston AD, Macdonald GA, Purdie DM, Prins JB, Ash S, et al. Effect of weight reduction on liver histology and biochemistry in patients with chronic hepatitis C. Gut 2002;51:89–94.

[26] Kato M, Miwa Y, Tajika M, Hiraoka T, Muto Y, Moriwaki H. Preferential use of branched-chain amino acids as an energy substrate in patients with liver cirrhosis. Intern Med 1998;37:429–34.

[27] Müller MJ, Böttcher J, Selberg O, Weselmann S, Böker KH, Schwarze M, et al. Hypermetabolism in clinically stable patients with liver cirrhosis. Am J Clin Nutr 1999;69:1194–201.

[28] Süttmann U, Ockenga J, Hoogestraat L, Selberg O, Schedel I, Deicher H, et al. Resting energy expenditure and weight loss in human immunodeficiency virus–infected patients. Metabolism 1993; 42:1173–9.

[29] Harris R, Benedict F. A biometric study of basal metabolism in man. Washington, DC: Carnegie Institute of Washington; 1919, p. 279.

[30] Moriwaki H, Aoyagi S, Ishizuka Y, Sasaki M, Santou K, Sugiyama M, et al. Japanese anthropometric reference data 2001. Osaka: Medical Review; 2002.

[31] Nakaya Y, Okita K, Suzuki K, Moriwaki H, Kato A, Miwa Y, et al. BCAA-enriched snack improves nutritional state of cirrhosis. Nutrition 2007;23:113–20.

[32] Mathur S, Peng S, Gane EJ, McCall JL, Plank LD. Hypermetabolism predicts reduced transplant-free survival independent of MELD and Child-Pugh scores in liver cirrhosis. Nutrition 2007;23:398–403.

[33] Shiraki M, Shimomura Y, Miwa Y, Fukushima H, Murakami T, Tamura T, et al. Activation of hepatic branched-chain alpha-keto acid dehydrogenase complex by tumor necrosis factor-alpha in rats. Biochem Biophys Res Commun 2005;328:973–8.

[34] Lin RS, Lee FY, Lee SD, Tsai YT, Lin HC, Lu RH, et al. Endotoxemia in patients with chronic liver diseases: relationship to severity of liver diseases, presence of esophageal varices, and hyperdynamic circulation. J Hepatol 1995;22:165–72.

[35] Gilles PN, Fey G, Chisari FV. Tumor necrosis factor alpha negatively regulates hepatitis B virus gene expression in transgenic mice. J Virol 1992;66:3955–60.

[36] Gilles PN, Guerrette DL, Ulevitch RJ, Schreiber RD, Chisari FV. HBsAg retention sensitizes the hepatocyte to injury by physiological concentrations of interferon-gamma. Hepatology 1992;16:655–63.